Delft University of Technology
Faculty of Electrical Engineering, Mathematics and Computer Science
Delft Institute of Applied Mathematics

Feasibility study of a tire hydroplaning simulation in a monolithic finite element code using a coupled Eulerian-Lagrangian method

A thesis submitted to the
Delft Institute of Applied Mathematics
in partial fulfillment of the requirements

for the degree

MASTER OF SCIENCE
in
APPLIED MATHEMATICS

by

ADRIAAN SILLEM

Delft, the Netherlands
June 2008

MSc THESIS APPLIED MATHEMATICS

"Feasibility study of a tire hydroplaning simulation in a monolithic finite element code using a coupled Eulerian-Lagrangian method"

Adriaan Sillem

Delft University of Technology

Daily supervisor

Dr.ir. A. Böhmer

Responsible professor

Prof.dr.ir. C. Vuik

Other thesis committee members

Prof.dr.ir. D.J. Rixen

June 2008

Delft, the Netherlands

GOODYEAR TECHNICAL CENTER

Feasibility study of a tire hydroplaning simulation in a monolithic finite element code using a coupled Eulerian-Lagrangian method

A. Sillem

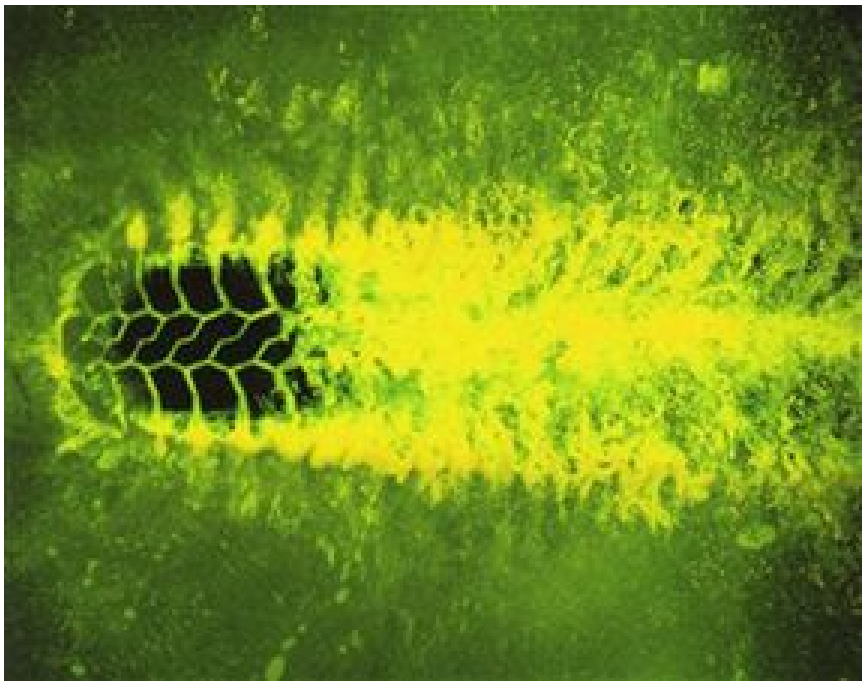

Preface

This is the interim report for (partially) the degree of Master of Science in Applied Mathematics, faculty of Electrical Engineering, Mathematics and Computer Science of the Delft University of Technology. It serves as documentation for the progress made during the graduation. The graduation is under supervision of division Numerical Analysis and has a duration of eight to nine months, equal to 42 European Credits (EC).

The graduation is carried out at the Goodyear Technical Center Luxembourg (GTC*L) in Colmar-Berg. This company is prominent in the worldwide production of tires for cars, trucks, airplanes and earth-movers. Purpose is to make a feasibility study of a tire hydroplaning simulation in a single FEA code using a coupled Eulerian-Lagrangian method. The concerning FEA code Abaqus 6.7-EF1 is provided by Simulia, Dassault Systèmes.

June 2008, Colmar-Berg

Adriaan Sillem

Goodyear Technical Center Luxembourg in Colmar-Berg.

Contents

List of Figures

Chapter 1

Hydroplaning

1.1 Phenomenon

Hydroplaning or aquaplaning by a road vehicle occurs when a layer of fluid builds up between the rubber tires of the vehicle and the road surface, leading to the loss of traction and thus preventing the vehicle from responding to control inputs such as steering, braking or accelerating. It becomes, in effect, an unpowered and unsteered sled.

Figure 1.1: hydroplaning.

Every vehicle function that changes the acceleration results in a load on the tires. Control of this load relies on the friction between the tire contact surface -also called the footprint- and the road surface.

The tread or grooves of a tire are designed to remove fluid from beneath the tire, providing friction with the road surface even in wet conditions. Hydroplaning occurs when a tire encounters more fluid than it can dissipate. Fluid pressure in front of the wheel forces a wedge of fluid under the leading edge of the tire, causing it to lift from the road. The tire then skates on a sheet of fluid with little, if any, direct road contact, resulting in loss of control.

Likelihood of hydroplaning increases with

- speed: in less time the same amount of fluid has to be dissipated
- depth of fluid: more depth increases fluid volume to be dissipated
- viscosity and mass of fluid: results in inertia in the dissipation of the fluid
- tread wear: the grooves are less deep and thus the volume available for fluid storage/transportation is less
- tire-wideness: narrower tires are less vulnerable to hydroplaning because the vehicle weight is distributed over a smaller footprint, resulting in a greater ability for the tires to push fluid out of the way. Also, the volume of the fluid to be dissipated is smaller for narrower tires.

The last item is the reason that bicycles, motorcycles and similar vehicles with an semi-elliptic cross-section are less likely to hydroplane. But while a slide in a four-wheeled vehicle is correctable with practice, the same slide on a motorcycle will generally cause the rider to fall, with severe consequences. Thus, despite the relative lack of hydroplaning danger, motorcycle riders must be even more cautious because overall traction is reduced by wet roads.

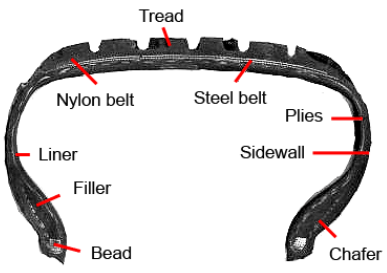

Figure 1.2: cross-section car tire.

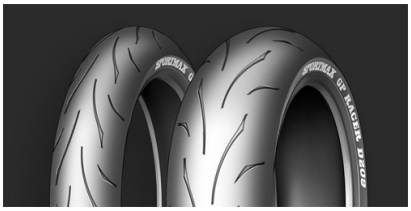

Figure 1.3: motorcycle tire.

1.2 Interest

Predicting hydroplaning has been a challenge for the tire industry. The speed at which a tire starts to hydroplane is a safety criterion.

With retrospect, improvements concerning hydroplaning were obtained experimentally. This is an expensive proces. A tread profile has to be designed. A mould design or laser cutting should realize this

profile. Afterwards it needs to be tested experimentally. Cost- and timewise, making improvements by simulation instead of empirism is more attractive.

Studies made on simulating hydroplaning are very rare. The results of the available studies are not useful or renewing. Because of this, it is only since the previous year that FEA program developers have made implementations that can eluminate the simulating of hydroplaning. Abaqus, Ansys and LS-Dyna are examples of these FEA programs. Still, these implementations are brand new and therefor need to be reviewed intensively before assuming an adequate solution is produced by it. On the issue of hydroplaning, GTC*L is on of the first to do this.

Figure 1.4: sprinkling the track for a hydrroplaning test.

Chapter 2

Definition of the problem

A rubber rotating tire with a tread profile enters a pond, cf. Figure 2.1. What does this seemingly simple sentence imply in modelling language?

Rubber is an elastomer and in general modeled as a viscoelastic and hyperelastic material, cf. 5.3. It is bonded to a carcass and belt package existing of anisotropic composites, see 5.3. The rotation of the tire implies a moving boundary for the fluid. This moving boundary has a tread profile which needs to be meshed for the finite element method (FEM) used for discretisation. The mesh can, depending on the reference frame, move with the material or be fixed in space, see 3 and 4.2. This also holds for the fluid. Fluid can also be discretised by the finite volume method (FVM) instead of the FEM. The gravitational load of the vehicle is transfered to the fluid by means of contact and to the internal energy of the rubber. Even simplified rolling contact has been a headcase for engineers [13]. Variation in the internal energy of rubber is accompanied with hysteresis effects, cf. 5.3. The transfer to the fluid results in an increase of the pressure. This transfer takes place over a moving boundary interface with on both sides different meshes. Depending on the tread profile, viscosity and density the fluid is dissipated with a certain speed and direction.

So a seemingly simple sentence gives, in modelling language, raise to a complex problem.

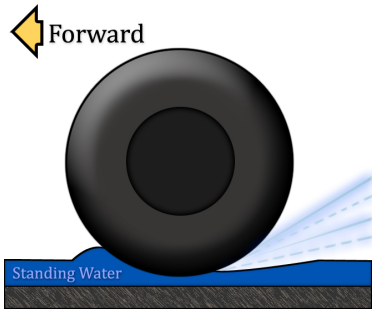

Figure 2.1: sideview hydroplaning.

Summarising, the modelling of hydroplaning can be split up in correlated issues:

- viscoelastic and hyperelastic rubber
- anisotropic composites
- moving boundary/interface
- discretisation with FEM or FVM
- reference frame
- mesh of tire
- mesh of fluid
- rolling contact
- information exchange over non-matching meshes
- fluid dynamics.

This characterization of hydroplaning implies it being an element of the class of fluid-structure interaction (FSI) problems. In this class of problems, tracking of the interface and transfer of information over the interface are the focal points. FSI and its link to hydroplaning is explained extensively in chapter 6.

Chapter 3

Discretisation mesh

3.1 Introduction

In the trend of fluid dynamics, simulating hydroplaning requires attention to mesh forming because of large gradients in the dynamics of the fluid. Both for the FEM and FVM.

There are several reference frames to be considered for mesh forming. Extent of deformation and movement are factors to be taken into account. Each frame has its own merits.

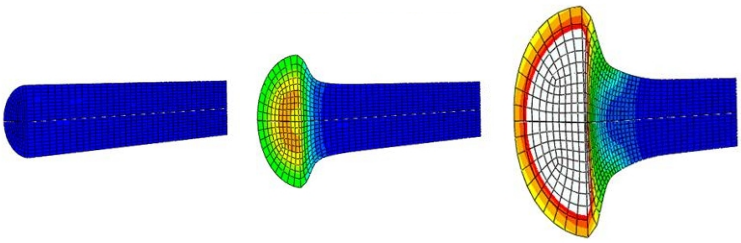

Figure 3.1: impact of a rod on a wall, large deformations, ALE meshed.

3.2 Eulerian formulation

An Eulerian frame is fixed in space. The considered domain is divided into elements. With deformation and movement, materials flow through the elements. Where high gradients are expected, a fine mesh is needed, see Figure 3.2. Advantages are that the mesh does not change per timestep and that large deformations do not increase the needed computation power. For this reason, the Eulerian frame is used widely in fluid dynamics. A disadvantage is that an interface is not tracked accurately, which is of importance with FSI problems.

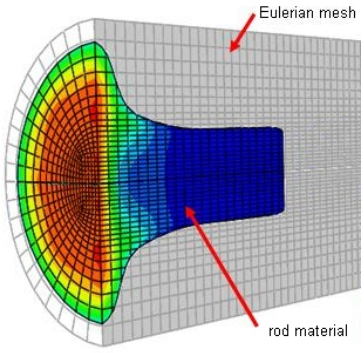

Figure 3.2: Eulerian mesh.

3.3 Lagrangian formulation

A Lagrangian frame moves with the material. In this way the interface of the material is tracked precisely, see Figure 3.3. Large deformations however, lead to mesh tangling implying a less precise solution. Remeshing is needed in this case, costing computational power. When considering materials with high E modulus, deformations are small and the Lagrangian frame is attractive. For this reason, the Lagrangian frame is used widely in structure mechanics.

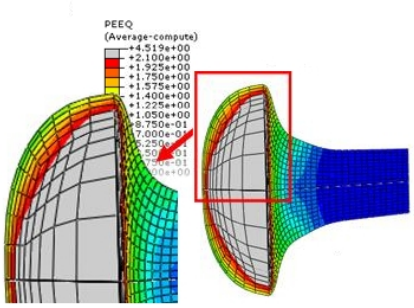

Figure 3.3: Lagrangian mesh.

3.4 Arbitrary Lagrangian-Eulerian formulation

Because of the shortcomings of purely Lagrangian and purely Eulerian descriptions, a technique has been developed that succeeds, to a certain extent, in combining the best features of both the Lagrangian and the Eulerian approaches. Such a technique is known as the arbitrary Lagrangian-Eulerian (ALE) description. In the ALE description, the nodes of the computational mesh may be moved with the continuum in normal Lagrangian fashion, or be held fixed in Eulerian manner, or be moved in some arbitrary specified way to give a continuous rezoning capability, see Figures 3.1 and 3.4. Because of this freedom in moving the computational mesh offered by the ALE description, greater distortions of the continuum can be handled than would be allowed by a purely Lagrangian method, with more resolution than that offered by a purely Eulerian approach. The mesh follows the boundary. However, this freedom in mesh movement has its limits. A treatment of mesh quality metrics and its limitations can be found in [3] and an extensive desciption of ALE methods can be found in [10].

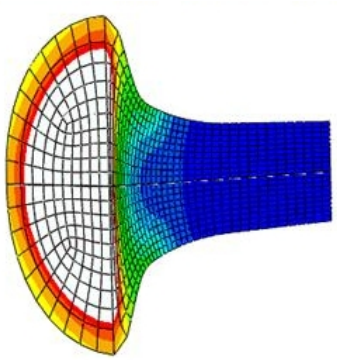

Figure 3.4: ALE mesh.

3.5 Coupled Eulerian-Lagrangian formulation

The coupled Eulerian-Lagrangian (CEL) method also attempts to capture the strenghts of the Lagrangian and Eulerian methods. In general, a Lagrangian frame is used to discretise the moving structure while an Eulerian frame is used to discretise the fluid domain. The boundary of the Lagrangian domain is taken to represent the interface between the different domains. Interface models use the velocity of the Lagrangian boundary as a kinematic constraint in the Eulerian calculation and the stress with the Eulerian cell to calculate the resulting surface stress on the Lagrangian domain [6]. Different CEL algorithms may be characterized by the details of how this interface condition is treated [14].

As the name clearly states, Abaqus' CEL method uses a CEL approach, see Figure 3.5. This method is used for the class of FSI problems, which involves large deformations. Details of their CEL meshing method are yet to be discovered and reviewed. The interface tracking method used in this FSI solver is discussed in 6.4.

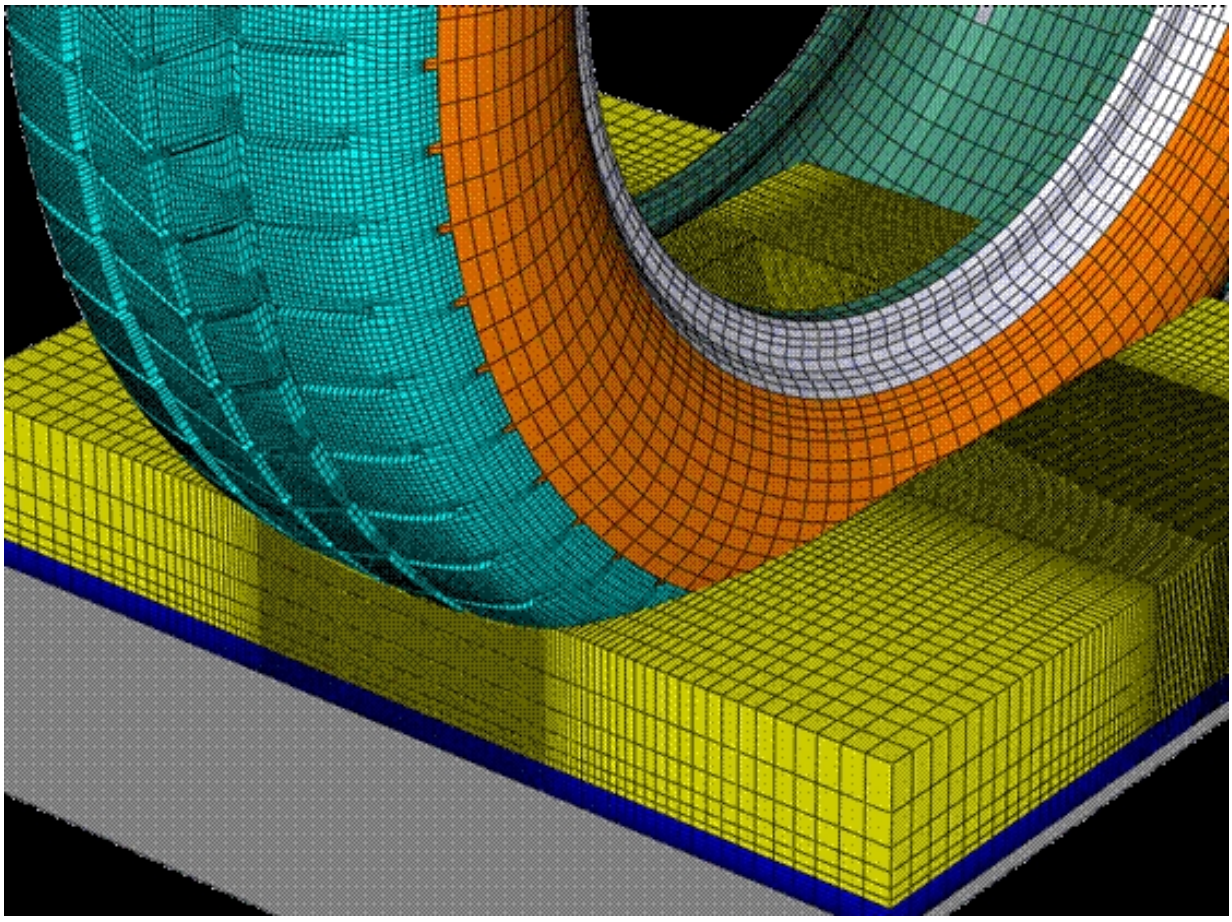

Figure 3.5: CEL mesh in Abaqus, Lagrangian structure and Eulerian fluid.

Chapter 4

Fluid dynamics

4.1 Introduction

Fluid dynamics is governed by three fundamental equations: the continuity, momentum and energy equation. They are the mathematical statements of three fundamental principles upon which all of fluid dynamics is based.

- Continuity from mass conservation.
- Momentum from Newton's second law $\boldsymbol{F} = m\boldsymbol{a}$.
- Energy equation from conservation of energy.

The deduction of these equations differs per reference frame and scale, which is shown in 4.3 for the conservation of mass. Although the reference frame and scale might differ, equivalence still holds, as shown in 4.3.5.

Considering hydroplaning, assumptions for the flow are made, changing the governing equations. Initial and boundary conditions are explained.

4.2 Reference frame and scale

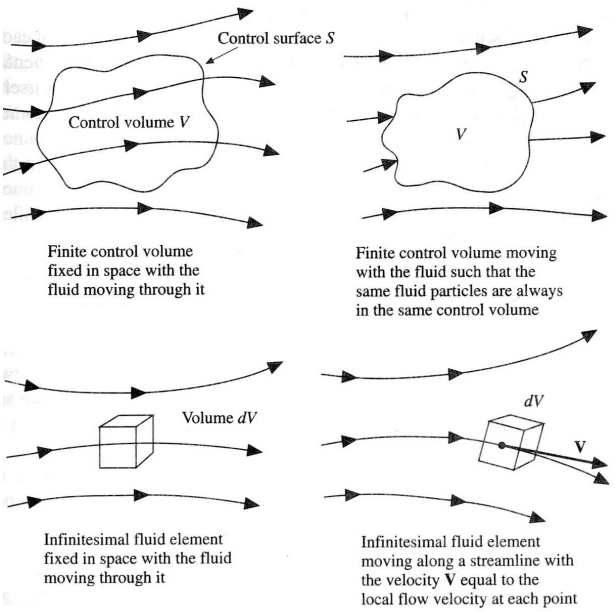

Figure 4.1: differences in frame and scale [11].

Problems in fluid dynamics can be considered on different scales and with different reference frames. The scale can be either continuum or an infinitesimal. The reference frame can be either fixed in space of moving with the fluid (Figure 4.1), called the Eulerian and Langrangian perspective respectively. The corresponding deduced equations are to be called in conservation and nonconservation form respectively. The latter denomination merely comes from the tradition of stating conservation laws relative to a fixed or Eulerian frame. In case of a Lagrangian domain a term is comprised in the substantial derivative (see 4.3.2), which makes it nonconservative. The fluid-flow equations that we directly obtain by applying the fundamental physical principles to a finite control volume are in integral form. These integral forms of the governing equations can be manipulated to obtain partial differential equations. This is shown in 4.3.5.

4.3 Conservation of mass

4.3.1 Continuum scale with fixed frame

Consider a control volume of arbitrary shape and of finite size fixed in space (Figure 4.1 upperleft). The fluid moves through the volume, across the surface. Mass conservation can in this case be described by

$$\begin{array}{rcl} \text{net mass flow out} & & \text{time rate of} \\ \text{of control volume} & = & \text{decrease of mass} \\ \text{through surface} & & \text{inside control volume} \end{array} .$$

The mass flow of a moving fluid across any fixed surface is equal to (density) $\times$ (area of surface) $\times$ (component of velocity perpendicular to the surface). Notice that the density is a function of space and time, so $\rho = \rho(x, y, z, t)$ in $[\frac{kg}{m^3}]$. In formula we have for the net mass flow out of the controle volume through surface $\partial V = S \subseteq \mathbb{R}^3$ in $[m^2]$

$$\iint_S \rho \boldsymbol{v} \cdot \boldsymbol{n} dS$$

with $\boldsymbol{v}, \boldsymbol{n} \in \mathbb{R}^3$ the velocity in $[\frac{m}{s}]$ and normal to the closed surface S respectively.

The time rate of decrease of mass inside volume $V \subseteq \mathbb{R}^3$ in $[m^3]$ is

$$-\frac{\partial}{\partial t} \iiint_V \rho dV.$$

It follows that

$$\iint_S \rho \boldsymbol{v} \cdot \boldsymbol{n} dS = -\frac{\partial}{\partial t} \iiint_V \rho dV$$

or

$$\iint_S \rho \boldsymbol{v} \cdot \boldsymbol{n} dS + \frac{\partial}{\partial t} \iiint_V \rho dV = 0. \tag{4.1}$$

Equation (4.1) is the integral form of mass conservation. The finite aspect of the control volume is the cause of the integral form.

4.3.2 Continuum scale with moving frame

Consider the model in Figure 4.1 in the upperright corner. Because the element is moving with the fluid, mass conservation is in this case

$$\frac{D}{Dt} \iiint_V \rho dV = 0. \tag{4.2}$$

Why is the derivative suddenly written as $\frac{D}{Dt}$ instead of the regular $\frac{\partial}{\partial t}$ you might ask? This is done to emphasize the difference of the space depending on time in this model, namely $\rho = \rho(x(t), y(t), z(t), t)$. This was not the case before. It is the differentation operator in time considering that during the time interval Dt the particles considered remain the same, even if they are moving as in the current model. With $x_1 = x$, $x_2 = y$ and $x_3 = z$ in $[m]$ as the prinicpal directions, denote

$$\begin{aligned} \frac{D}{Dt} &= \left.\frac{\partial}{\partial t}\right|_{\text{given particle}} \\ &= \left.\frac{\partial}{\partial t}\right|_{\text{given space position}} + \sum_{i=1}^{3} \left.\frac{\partial x_i}{\partial t}\right|_{\text{given particle}} \frac{\partial}{\partial x_i} \end{aligned} \tag{4.3}$$

called the material or substantial derivative. For the density we would get

$$\begin{aligned} \frac{D}{Dt}\rho(x(t), y(t), z(t), t) &= \left.\frac{\partial}{\partial t}\rho(x(t), y(t), z(t), t)\right|_{\text{given particle}} \\ &= \frac{\partial \rho}{\partial t} + \frac{\partial \rho}{\partial x}\frac{\partial x}{\partial t} + \frac{\partial \rho}{\partial y}\frac{\partial y}{\partial t} + \frac{\partial \rho}{\partial z}\frac{\partial z}{\partial t} \\ &= \frac{\partial \rho}{\partial t} + \boldsymbol{\nabla}\rho \cdot \boldsymbol{v}. \end{aligned}$$

Note that this can be seen as the chain rule.

4.3.3 Infinitesimal scale with fixed frame

Consider the model in Figure 4.1 in the lowerleft corner. Analogous to the model with a finite size and fixed frame, recall that

$$\begin{array}{lcl} \text{net mass flow out} & & \text{time rate of} \\ \text{of control volume} & = & \text{decrease of mass} \\ \text{through surface } S & & \text{inside control volume} \end{array} .$$

The net mass flow out is equal to (density) × (area of surface) × (component of velocity perpendicular to the surface). Because the infintesimal element is a cube, considering directions is simplified compared to the continuum scale. Normal $\boldsymbol{n}$ is superfluous, considering the x, y and z direction seperately is sufficient. Net outflow in x direction is

$$(\rho u)|_{x+dx} dydz - (\rho u)|_x dydz$$

Taylor expansion of $(\rho u)|_{x+dx}$ around x gives

$$(\rho u)|_{x+dx} = \sum_{n=0}^{\infty} \frac{(dx)^n}{n!} \left. \frac{\partial^n (\rho u)}{\partial x^n} \right|_x .$$

Because dx is infinitesimal, we can neglect the higher order terms to get $(\rho u)|_x + dx \left. \frac{\partial(\rho u)}{\partial x} \right|_x$. Herewith, the net outflow in x direction becomes (cf. Figure 4.2)

$$\begin{aligned} (\rho u)|_{x+dx} dydz - (\rho u)|_x dydz &= \left[(\rho u)|_x + dx \left. \frac{\partial(\rho u)}{\partial x} \right|_x \right] dydz - (\rho u)|_x dydz \\ &= \left. \frac{\partial(\rho u)}{\partial x} \right|_x dxdydz. \end{aligned}$$

Analogous we have in the y and z direction

$$\begin{aligned} (\rho v)|_{y+dy} dxdz - (\rho v)|_y dxdz &= \left. \frac{\partial(\rho v)}{\partial y} \right|_y dxdydz \\ (\rho w)|_{z+dz} dxdy - (\rho w)|_z dxdy &= \left. \frac{\partial(\rho w)}{\partial z} \right|_z dxdydz. \end{aligned}$$

Furthermore

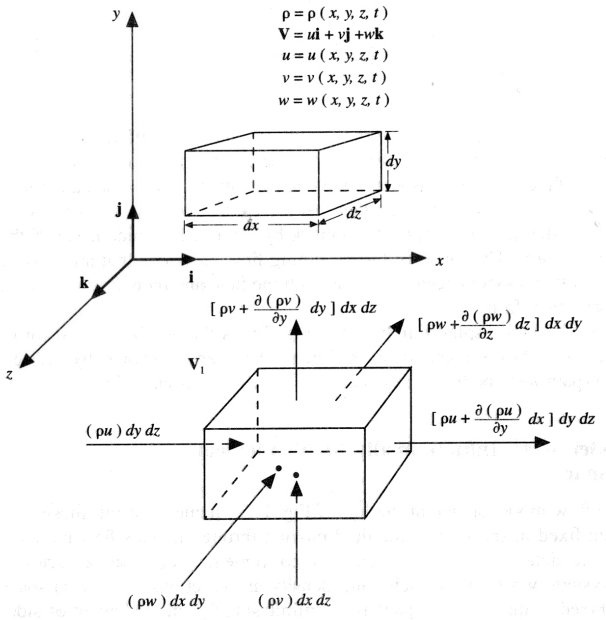

Figure 4.2: model of an infitesimal small element fixed in space [11].

$$\text{time rate of mass decrease} = -\frac{\partial \rho}{\partial t} dxdydz.$$

Notice that the density ρ can be assumed constant in space as the element is infinitesimal.

Hence, we get

$$\begin{aligned}(\frac{\partial(\rho u)}{\partial x}\Big|_x + \frac{\partial(\rho v)}{\partial y}\Big|_y + \frac{\partial(\rho w)}{\partial z}\Big|_z)dxdydz &= -\frac{\partial \rho}{\partial t}dxdydz \\ (\frac{\partial(\rho u)}{\partial x}\Big|_x + \frac{\partial(\rho v)}{\partial y}\Big|_y + \frac{\partial(\rho w)}{\partial z}\Big|_z) &= -\frac{\partial \rho}{\partial t}\end{aligned}$$

leading to

$$\frac{\partial \rho}{\partial t} + \boldsymbol{\nabla} \cdot (\rho \boldsymbol{v}) = 0. \tag{4.4}$$

4.3.4 Infinitesimal scale with moving frame

Consider the model in Figure 4.1 in the lower-right corner. An infintesimal fluid element moving with the flow. This element has a fixed mass, but in general its shape and volume will change as it moves downstream. Denote the fixed mass and variable volume of this element by δm and δV respectively:

$$\delta m = \rho \delta V.$$

Analogous with the continuum scale case, the rate of change of the mass in time is equal to zero. The element is moving with the fluid so we again use the notation of the material derivative:

$$\begin{aligned}\frac{D(\delta m)}{Dt} &= 0 \\ \frac{D(\rho \delta V)}{Dt} &= 0 \\ \delta V \frac{D\rho}{Dt} + \rho \frac{D(\delta V)}{Dt} &= 0 \\ \frac{D\rho}{Dt} + \frac{\rho}{\delta V}\frac{D(\delta V)}{Dt} &= 0\end{aligned}$$

From the physical meaning of the divergence we have $\frac{1}{\delta V}\frac{D(\delta V)}{Dt} = \boldsymbol{\nabla} \cdot \boldsymbol{v}$ [11]. Thus

$$\frac{D\rho}{Dt} + \rho \boldsymbol{\nabla} \cdot \boldsymbol{v} = 0. \tag{4.5}$$

4.3.5 Equivalence of the equations

We deduced equations (4.1), (4.2), (4.4) and (4.5); these are four equations either in integral or partial differential form, for either the conservative or nonconservative case (cf. Figure 4.3). But in a way, they are all equivalent. An important difference is that the integral forms allow the presence of discontinuities inside the fixed control volume, whereas the partial differential forms assume first order differentiability, implying continuity. The integral form is therefor considered to be more fundamental then partial differential form.

We will deduce (4.5) from (4.4), (4.4) from (4.1) and (4.1) from (4.2) to prove that every equation can be rewritten in each of the remaining three equations. So we start with

$$\frac{D}{Dt}\iiint_V \rho dV = 0.$$

Since the material derivative itself represents a time rate of change associated with a moving element and the limits on the volume integral in (4.2) are determined by these same moving elements, the material

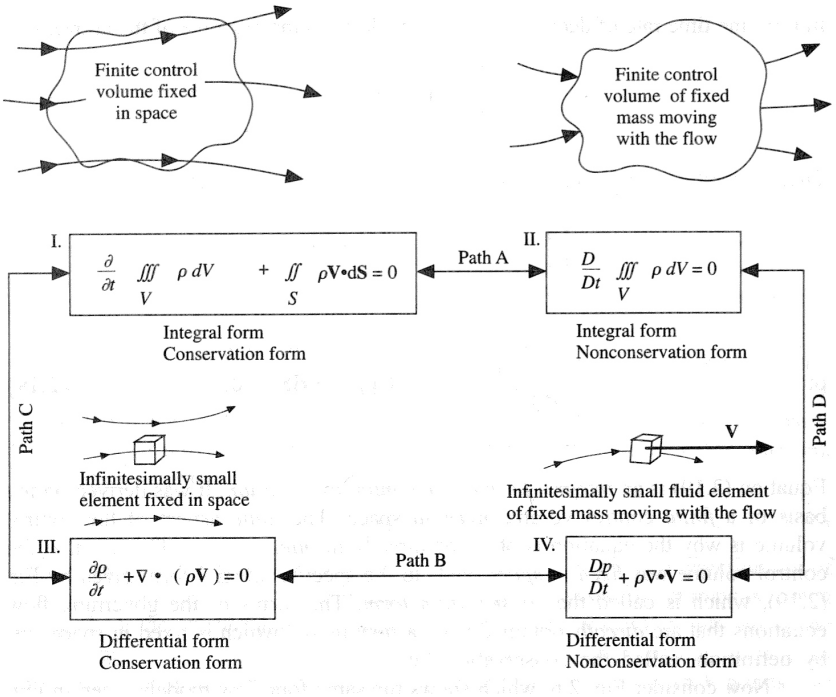

Figure 4.3: different forms of the continuity equation [11].

derivative can be taken inside the integral.

$$
\begin{aligned}
\iiint_V \frac{D(\rho dV)}{Dt} &= 0 && \text{product-rule}\\
\iiint_V \frac{D\rho}{Dt} dV + \iiint_V \rho \frac{D(dV)}{Dt} &= 0 && \text{multiplicate by } \frac{dV}{dV} = 1\\
\iiint_V \frac{D\rho}{Dt} dV + \iiint_V \rho \left[\frac{1}{dV}\frac{D(dV)}{Dt}\right] dV &= 0 && \text{equivalence } \frac{1}{\delta V}\frac{D(\delta V)}{Dt} = \boldsymbol{\nabla}\cdot\boldsymbol{v}\\
\iiint_V \frac{D\rho}{Dt} dV + \iiint_V \rho\boldsymbol{\nabla}\cdot\boldsymbol{v} dV &= 0 && (4.3)\\
\iiint_V \left[\frac{\partial \rho}{\partial t} + \boldsymbol{v}\cdot\boldsymbol{\nabla}\rho\right] dV + \iiint_V \rho\boldsymbol{\nabla}\cdot\boldsymbol{v} dV &= 0\\
\iiint_V \left[\frac{\partial \rho}{\partial t} + \boldsymbol{v}\cdot\boldsymbol{\nabla}\rho + \rho\boldsymbol{\nabla}\cdot\boldsymbol{v}\right] dV &= 0 && \text{product-rule}\\
\iiint_V \left[\frac{\partial \rho}{\partial t} + \boldsymbol{\nabla}\cdot(\rho\boldsymbol{v})\right] dV &= 0 && \text{divergence theorem}\\
\iiint_V \frac{\partial \rho}{\partial t} dV + \iint_S \rho\boldsymbol{v}\cdot\boldsymbol{n} dS &= 0 && \boldsymbol{v} \text{ independent of } t\\
\frac{\partial}{\partial t}\iiint_V \rho dV + \iint_S \rho\boldsymbol{v}\cdot\boldsymbol{n} dS &= 0
\end{aligned}
$$

The last equation corresponds with (4.1).

A proof of the divergence theorem $\iiint_V \boldsymbol{\nabla}\cdot\boldsymbol{v} dV = \iint_S \boldsymbol{v}\cdot\boldsymbol{n} dS, \boldsymbol{v} \in \mathbb{R}^3$ can be found in [18].

Along the deduction we encountered $\iiint_V \left[\frac{\partial \rho}{\partial t} + \boldsymbol{\nabla}\cdot(\rho\boldsymbol{v})\right] dV = 0$. Since the volume is arbitrarily drawn in space, the only way for the integral to be equal to zero is if

$$\frac{\partial \rho}{\partial t} + \boldsymbol{\nabla}\cdot(\rho\boldsymbol{v}) = 0$$

which corresponds with (4.4).

The equivalence of (4.4) and (4.5) follows from application of the product and chain rules:

$$
\begin{aligned}
\frac{\partial \rho}{\partial t} + \boldsymbol{\nabla}\cdot(\rho\boldsymbol{v}) &= 0\\
\frac{\partial \rho}{\partial t} + \boldsymbol{v}\cdot\boldsymbol{\nabla}\rho + \rho\boldsymbol{\nabla}\cdot\boldsymbol{v} &= 0\\
\frac{D\rho}{Dt} + +\rho\boldsymbol{\nabla}\cdot\boldsymbol{v} &= 0.
\end{aligned}
$$

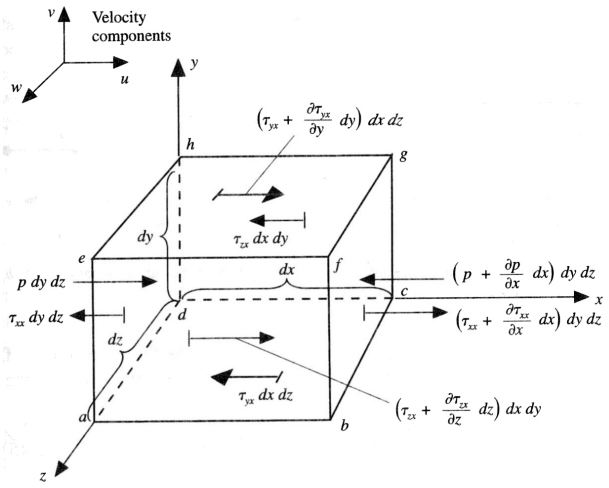

Figure 4.4: forces in x direction [11].

4.4 Conservation of momentum

Newton's second law states $\boldsymbol{F} = m\boldsymbol{a}$. When considering a moving infinitesimal fluid element, it can experience body and/or surface forces.

- Body forces, which act directly on the volumetric mass of the fluid element. These forces "act at a distance"; examples can be gravitational and electromagnetic forces.

- Surface forces, which act directly on the surface of the fluid element. They are due only to two sources.

  - The pressure distribution acting on the surface, imposed by the outside fluid surrounding the fluid element.

  - The shear and normal stress distributions acting on the surface, also imposed by the outside fluid by means of friction.

Let $\boldsymbol{f}$ denote the body force per unit mass in $[\frac{N}{kg}]$, then

$$\text{body force on element} = \rho \boldsymbol{f} dxdydz.$$

From Figure 4.4 it follows that

$$\begin{aligned}
\text{net surface force in } x \text{ direction} &= \left[p - \left(p + \frac{\partial p}{\partial x}dx\right)\right] dydz + \left[\left(\tau_{xx} + \frac{\partial \tau_{xx}}{\partial x}dx\right) - \tau_{xx}\right] dydz \\
&+ \left[\left(\tau_{yx} + \frac{\partial \tau_{yx}}{\partial y}dy\right) - \tau_{yx}\right] dxdz + \left[\left(\tau_{zx} + \frac{\partial \tau_{zx}}{\partial z}dz\right) - \tau_{zx}\right] dxdy \\
&= \left[-\frac{\partial p}{\partial x} + \frac{\partial \tau_{xx}}{\partial x} + \frac{\partial \tau_{yx}}{\partial y} + \frac{\partial \tau_{zx}}{\partial z}\right] dxdydz
\end{aligned}$$

Note that the first index of stress τ in $[Pa]$ denotes the orientation of the surface normal and the second the direction of the stress. The pressure p is in $[Pa]$. The $\star + \frac{\partial \star}{\partial\{x,y,z\}} d\{x,y,z\}$ terms are again from Taylor expansions, analogous with the decuction in 4.3.3. In fact, this method is used throughout all deductions on infinitesimal scale.

With analogy in y and z direction, the total force becomes

$$\begin{aligned}
\boldsymbol{F} &= \left[\rho\boldsymbol{f} - \boldsymbol{\nabla}p + \begin{pmatrix} \frac{\partial\tau_{xx}}{\partial x} + \frac{\partial\tau_{yx}}{\partial y} + \frac{\partial\tau_{zx}}{\partial z} \\ \frac{\partial\tau_{xy}}{\partial x} + \frac{\partial\tau_{yy}}{\partial y} + \frac{\partial\tau_{zy}}{\partial z} \\ \frac{\partial\tau_{xz}}{\partial x} + \frac{\partial\tau_{yz}}{\partial y} + \frac{\partial\tau_{zz}}{\partial z} \end{pmatrix}\right] dxdydz \\
&= \left[\rho\boldsymbol{f} - \boldsymbol{\nabla}p + \left\{ \begin{pmatrix} \frac{\partial}{\partial x} & \frac{\partial}{\partial y} & \frac{\partial}{\partial z} \end{pmatrix} \underbrace{\begin{pmatrix} \tau_{xx} & \tau_{xy} & \tau_{xz} \\ \tau_{yx} & \tau_{yy} & \tau_{yz} \\ \tau_{zx} & \tau_{yz} & \tau_{zz} \end{pmatrix}}_{=\boldsymbol{\tau}} \right\}^T\right] dxdydz \\
&= \left[\rho\boldsymbol{f} - \boldsymbol{\nabla}p + (\boldsymbol{\nabla}^T\boldsymbol{\tau})^T\right] dxdydz \\
&= \left[\rho\boldsymbol{f} - \boldsymbol{\nabla}p + \boldsymbol{\tau}^T\boldsymbol{\nabla}\right] dxdydz
\end{aligned}$$

With $\boldsymbol{F} = m\boldsymbol{a}$ and noting that $m = \rho dxdydz$, $\boldsymbol{a} = \frac{D\boldsymbol{v}}{Dt}$ and for the stress tensor $\boldsymbol{\tau} = \boldsymbol{\tau}^T$ we get

$$\begin{aligned}
\left[\rho\boldsymbol{f} - \boldsymbol{\nabla}p + \boldsymbol{\tau}\boldsymbol{\nabla}\right] dxdydz &= \rho\frac{D\boldsymbol{v}}{Dt} dxdydz \\
\rho\boldsymbol{f} - \boldsymbol{\nabla}p + \boldsymbol{\tau}\boldsymbol{\nabla} &= \rho\frac{D\boldsymbol{v}}{Dt}
\end{aligned} \tag{4.6}$$

which are the Navier-Stokes equations in nonconservation form. The term $\boldsymbol{\tau}\boldsymbol{\nabla}$ is denoted with slight abuse of notation because it is routine to write the operator, in this case the $\boldsymbol{\nabla}$ operator, at the front of the term. In that case the term would look like $(\boldsymbol{\nabla}^T\boldsymbol{\tau})^T$, as denoted earlier above. The term is often written simply as $\boldsymbol{\nabla}\boldsymbol{\tau}$, neglecting the correctness of the matrix dimensions and assuming the $\boldsymbol{\nabla}$ operator is in row form instead of the regular column form. Throughout this report the notation $\boldsymbol{\tau}\boldsymbol{\nabla}$ will be maintained, respecting the matrix dimensions. Furthermore, in $\boldsymbol{a} = \frac{D\boldsymbol{v}}{Dt}$ the material derivative is used because the velocity $\boldsymbol{v}$ can be relative to a fixed or moving frame.

Writing out the material derivative gives the conservation form

$$\begin{aligned}
\rho\boldsymbol{f} - \boldsymbol{\nabla}p + \boldsymbol{\tau}\boldsymbol{\nabla} &= \rho\frac{D\boldsymbol{v}}{Dt} \\
\rho\boldsymbol{f} - \boldsymbol{\nabla}p + \boldsymbol{\tau}\boldsymbol{\nabla} &= \rho\left(\frac{\partial\boldsymbol{v}}{\partial t} + (\boldsymbol{v}\cdot\boldsymbol{\nabla})\boldsymbol{v}\right)
\end{aligned} \tag{4.7}$$

where the notation $\boldsymbol{v}\cdot\boldsymbol{\nabla} = u\frac{\partial}{\partial x} + v\frac{\partial}{\partial y} + w\frac{\partial}{\partial z}$ is a scalar operator called the advective operator. This is with slight abuse of notation because an inner-product, and thus also the standard inner-product $\cdot$, is commutative by definition [17]. By definition $\boldsymbol{v}\cdot\boldsymbol{\nabla} = \boldsymbol{\nabla}\cdot\boldsymbol{v} = \frac{\partial u}{\partial x} + \frac{\partial v}{\partial y} + \frac{\partial w}{\partial z} \neq u\frac{\partial}{\partial x} + v\frac{\partial}{\partial y} + w\frac{\partial}{\partial z} = \boldsymbol{v}\cdot\boldsymbol{\nabla}$. This abuse is a result of the fact that $\boldsymbol{\nabla}$ is a vector operator - a vector whose elements are operators - and not a vector.

The terms $-\boldsymbol{\nabla}p + \boldsymbol{\tau}\boldsymbol{\nabla}$ are referred to as the Cauchy stress tensor, also written as

$$\begin{aligned}
-\boldsymbol{\nabla}p + \boldsymbol{\tau}\boldsymbol{\nabla} &= \left((-\boldsymbol{\nabla}p)^T\right)^T + \left((\boldsymbol{\tau}\boldsymbol{\nabla})^T\right)^T \\
&= \left(-\boldsymbol{\nabla}^T p\right)^T + \left(\boldsymbol{\nabla}^T\boldsymbol{\tau}^T\right)^T \\
&= \left(-\boldsymbol{\nabla}^T p + \boldsymbol{\nabla}^T\boldsymbol{\tau}^T\right)^T \\
&= \left(\boldsymbol{\nabla}^T(-p\boldsymbol{I} + \boldsymbol{\tau}^T)\right)^T \\
&= (-p\boldsymbol{I} + \boldsymbol{\tau}^T)^T\left((\boldsymbol{\nabla})^T\right)^T \\
&= (\underbrace{-p\boldsymbol{I}}_{\text{volumetric}} + \underbrace{\boldsymbol{\tau}}_{\text{deviatoric}})\boldsymbol{\nabla}
\end{aligned}$$

where $-p\boldsymbol{I}$ and $\boldsymbol{\tau}$ are the volumetric and deviatoric parts respectively of the Cauchy stress tensor. The deviatoric part is dependent of the material in question.

4.5 Conservation of energy

The physical principle stated in this section is merely the first law of thermodynamics, namely

$$\begin{array}{lcll} \text{rate of change} & & \text{net flux of} & \text{rate of work done on} \\ \text{of energy inside} & = & \text{heat into} & + \quad \text{element due to} \quad . \\ \text{fluid element} & & \text{element} & \text{body and surface forces} \end{array} \tag{4.8}$$

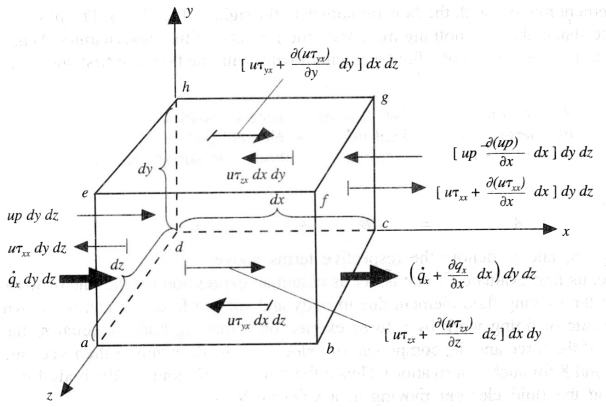

Figure 4.5: energy fluxes in x direction [11].

4.5.1 Rate of work due to body and surface forces

We first evaluate the rate of work due to forces. Again, we make difference between body and surface forces. For body forces we have

$$\text{rate of work done by body forces} = \rho \boldsymbol{f} \cdot \boldsymbol{v} dxdydz. \tag{4.9}$$

Analogous with the deduction in 4.3.3, 4.4 and with the help of Figure 4.5 we obtain the surface forces in x, y and z direction respectively:

$$\begin{aligned}
\text{rate of work done by surface forces} &= \Bigg[\underbrace{-\frac{\partial(up)}{\partial x} + \frac{\partial(u\tau_{xx})}{\partial x} + \frac{\partial(u\tau_{yx})}{\partial y} + \frac{\partial(u\tau_{zx})}{\partial z}}_{x \text{ direction}} + \underbrace{-\frac{\partial(vp)}{\partial y} + \frac{\partial(v\tau_{xy})}{\partial x} + \frac{\partial(v\tau_{yy})}{\partial y} + \frac{\partial(v\tau_{zy})}{\partial z}}_{y \text{ direction}} \\
&+ \underbrace{-\frac{\partial(wp)}{\partial z} + \frac{\partial(w\tau_{xz})}{\partial x} + \frac{\partial(w\tau_{yz})}{\partial y} + \frac{\partial(w\tau_{zz})}{\partial z}}_{z \text{ direction}} \Bigg] dxdydz \\
&= \left[-\boldsymbol{\nabla} \cdot p\boldsymbol{v} + \boldsymbol{\nabla} \cdot u \begin{pmatrix} \tau_{xx} \\ \tau_{yx} \\ \tau_{zx} \end{pmatrix} + \boldsymbol{\nabla} \cdot v \begin{pmatrix} \tau_{xy} \\ \tau_{yy} \\ \tau_{zy} \end{pmatrix} + \boldsymbol{\nabla} \cdot w \begin{pmatrix} \tau_{xz} \\ \tau_{yz} \\ \tau_{zz} \end{pmatrix} \right] dxdydz \\
&= \left[-\boldsymbol{\nabla} \cdot p\boldsymbol{v} + \boldsymbol{\nabla} \cdot \left\{ u \begin{pmatrix} \tau_{xx} \\ \tau_{yx} \\ \tau_{zx} \end{pmatrix} + v \begin{pmatrix} \tau_{xy} \\ \tau_{yy} \\ \tau_{zy} \end{pmatrix} + w \begin{pmatrix} \tau_{xz} \\ \tau_{yz} \\ \tau_{zz} \end{pmatrix} \right\} \right] dxdydz \\
&= \left[-\boldsymbol{\nabla} \cdot p\boldsymbol{v} + \boldsymbol{\nabla} \cdot \left\{ (u \quad v \quad w) \begin{pmatrix} \tau_{xx} & \tau_{yx} & \tau_{zx} \\ \tau_{xy} & \tau_{yy} & \tau_{zy} \\ \tau_{xz} & \tau_{yz} & \tau_{zz} \end{pmatrix} \right\}^T \right] dxdydz \\
&= \left[-\boldsymbol{\nabla} \cdot p\boldsymbol{v} + \boldsymbol{\nabla} \cdot \left(\boldsymbol{v}^T \boldsymbol{\tau}^T \right)^T \right] dxdydz \\
&= \left[-\boldsymbol{\nabla} \cdot p\boldsymbol{v} + \boldsymbol{\nabla} \cdot (\boldsymbol{\tau}\boldsymbol{v}) \right] dxdydz
\end{aligned} \tag{4.10}$$

4.5.2 Net flux of heat

The net flux of heat into the element is due to

- volumetric heating such as absorption or emission of radiation
- heat transfer across the surface due to temperature gradients, i.e. conduction.

Phenomena that result in volumetric heating are beyond the scope of this thesis and will therefor not be treated.

We obtain from Figure 4.5

$$\begin{aligned}
\text{heating of element by conduction} &= -\left(\frac{\partial q_x}{\partial x} + \frac{\partial q_y}{\partial y} + \frac{\partial q_z}{\partial z} \right) dxdydz \\
&= -\boldsymbol{\nabla} \cdot \boldsymbol{q} dxdydz
\end{aligned} \tag{4.11}$$

with $\boldsymbol{q} = (q_x \quad q_y \quad q_z)^T$ the flux of energy in $[\frac{J}{m^2 \cdot s}]$.

4.5.3 Rate of change of energy

The fluid element has two contributions to its total energy E in $[\frac{J}{kg}] = [\frac{m^2}{s^2}]$:

- the internal energy due to random molecular motion, e in $[\frac{J}{kg}]$
- the kinetic energy due to translational motion, $\frac{v^2}{2}$ in $[\frac{J}{kg}]$.

The mass of the element is $\rho dxdydz$ and we get the time rate of change by the operator $\frac{D}{Dt}$. Herewith

$$\text{time rate of change of energy inside element} = \rho \frac{D}{Dt}\left(e + \frac{v^2}{2}\right) dxdydz. \tag{4.12}$$

4.5.4 The energy equation

With (4.9) to (4.12), (4.8) becomes

$$\begin{aligned} \rho \frac{D}{Dt}\left(\underbrace{e + \frac{v^2}{2}}_{\text{total energy}}\right) dxdydz &= \left[\underbrace{-\boldsymbol{\nabla} \cdot \boldsymbol{q}}_{\text{conduction}} + \underbrace{\rho \boldsymbol{f} \cdot \boldsymbol{v}}_{\text{body forces}} \underbrace{-\boldsymbol{\nabla} \cdot p\boldsymbol{v} + \boldsymbol{\nabla} \cdot (\boldsymbol{\tau}\boldsymbol{v})}_{\text{surface forces}}\right] dxdydz \\ \rho \frac{D}{Dt}\left(e + \frac{v^2}{2}\right) &= \rho \boldsymbol{f} \cdot \boldsymbol{v} + \boldsymbol{\nabla} \cdot (\boldsymbol{\tau}\boldsymbol{v} - \boldsymbol{q} - p\boldsymbol{v}) \end{aligned} \tag{4.13}$$

which is the nonconservation form. Again, writing out the material derivative gives the conservation form

$$\rho\left[\frac{\partial}{\partial t}\left(e + \frac{v^2}{2}\right) + \boldsymbol{v} \cdot \boldsymbol{\nabla}\left(e + \frac{v^2}{2}\right)\right] = \rho \boldsymbol{f} \cdot \boldsymbol{v} + \boldsymbol{\nabla} \cdot (\boldsymbol{\tau}\boldsymbol{v} - \boldsymbol{q} - p\boldsymbol{v}) \tag{4.14}$$

4.6 Additional relations

The conservation of mass, momentum and energy form a set of five relations to determine ρ, $\boldsymbol{v}$ and e. However, there are still other unknowns such as p, $\boldsymbol{\tau}$ and $\boldsymbol{q}$. The following equations have to be taken into account to solve the system.

4.6.1 Shear stresses

In many applications, it is assumed that the fluid is Newtonian which means that

$$\tau_{xx} = \sigma_x = \lambda \boldsymbol{\nabla} \cdot \boldsymbol{v} + 2\mu \frac{\partial u}{\partial x} \tag{4.15}$$

$$\tau_{yy} = \sigma_y = \lambda \boldsymbol{\nabla} \cdot \boldsymbol{v} + 2\mu \frac{\partial v}{\partial y} \tag{4.16}$$

$$\tau_{zz} = \sigma_z = \lambda \boldsymbol{\nabla} \cdot \boldsymbol{v} + 2\mu \frac{\partial w}{\partial z} \tag{4.17}$$

$$\tau_{xy} = \tau_{yx} = \mu\left(\frac{\partial v}{\partial x} + \frac{\partial u}{\partial y}\right) \tag{4.18}$$

$$\tau_{xz} = \tau_{zx} = \mu\left(\frac{\partial u}{\partial z} + \frac{\partial w}{\partial x}\right) \tag{4.19}$$

$$\tau_{yz} = \tau_{zy} = \mu\left(\frac{\partial w}{\partial y} + \frac{\partial v}{\partial z}\right) \tag{4.20}$$

where μ is the molecular viscosity coeffcient and λ is the second viscosity coeffcient, both in $[Pa \cdot s]$. Stokes made the hypothesis that

$$\lambda = -\frac{2}{3}\mu \tag{4.21}$$

which is frequently used but to the present day not confirmed.

With the assumption of Newtonian fluid, the stress tensor $\boldsymbol{\tau}$ can be written as

$$\begin{aligned}
\boldsymbol{\tau} &= \begin{pmatrix} -\frac{2}{3}\mu\boldsymbol{\nabla}\cdot\boldsymbol{v}+2\mu\frac{\partial u}{\partial x} & \mu\left(\frac{\partial v}{\partial x}+\frac{\partial u}{\partial y}\right) & \mu\left(\frac{\partial u}{\partial z}+\frac{\partial w}{\partial x}\right) \\ \mu\left(\frac{\partial v}{\partial x}+\frac{\partial u}{\partial y}\right) & -\frac{2}{3}\mu\boldsymbol{\nabla}\cdot\boldsymbol{v}+2\mu\frac{\partial v}{\partial y} & \mu\left(\frac{\partial w}{\partial y}+\frac{\partial v}{\partial z}\right) \\ \mu\left(\frac{\partial u}{\partial z}+\frac{\partial w}{\partial x}\right) & \mu\left(\frac{\partial w}{\partial y}+\frac{\partial v}{\partial z}\right) & -\frac{2}{3}\mu\boldsymbol{\nabla}\cdot\boldsymbol{v}+2\mu\frac{\partial w}{\partial z} \end{pmatrix} \\
&= 2\mu\begin{pmatrix} \frac{-\boldsymbol{\nabla}\cdot\boldsymbol{v}}{3}+\frac{\partial u}{\partial x} & \frac{1}{2}\left(\frac{\partial v}{\partial x}+\frac{\partial u}{\partial y}\right) & \frac{1}{2}\left(\frac{\partial u}{\partial z}+\frac{\partial w}{\partial x}\right) \\ \frac{1}{2}\left(\frac{\partial v}{\partial x}+\frac{\partial u}{\partial y}\right) & \frac{-\boldsymbol{\nabla}\cdot\boldsymbol{v}}{3}+\frac{\partial v}{\partial y} & \frac{1}{2}\left(\frac{\partial w}{\partial y}+\frac{\partial v}{\partial z}\right) \\ \frac{1}{2}\left(\frac{\partial u}{\partial z}+\frac{\partial w}{\partial x}\right) & \frac{1}{2}\left(\frac{\partial w}{\partial y}+\frac{\partial v}{\partial z}\right) & \frac{-\boldsymbol{\nabla}\cdot\boldsymbol{v}}{3}+\frac{\partial w}{\partial z} \end{pmatrix} \\
&= 2\mu\left(\frac{-\boldsymbol{\nabla}\cdot\boldsymbol{v}}{3}\boldsymbol{I}+\frac{1}{2}\left[\boldsymbol{\nabla}\boldsymbol{v}^T+(\boldsymbol{\nabla}\boldsymbol{v}^T)^T\right]\right) \\
&:= 2\mu\boldsymbol{D}
\end{aligned} \tag{4.22}$$

which will be of importance in 4.7.4 with non-dimensionalising. The dimension of $\boldsymbol{D}$ is $[\frac{1}{s}]$.

4.6.2 Fourier's law

The heat flux $\boldsymbol{q}$ is related to the space variation of the temperature T in $[K]$. Fourier's law states that the heat flux is given by

$$\boldsymbol{q} = -k\boldsymbol{\nabla}T \tag{4.23}$$

where k in $[\frac{W}{m\cdot K}]$ is the coefficient of thermal conductivity.

4.6.3 Equations of state

There are still two relations needed to fully determine the fluid behaviour: the equations of state (EOS). Choosing ρ and e as independent variables, the EOS must provide

$$\begin{aligned} p &= p(e,\rho) \\ T &= T(e,\rho) \end{aligned} \tag{4.24}$$

Some usual EOS:

- incompressible fluid

$$\begin{aligned} \rho &= \text{constant} \\ e &= c_pT = c_VT \end{aligned}$$

- perfect gas and constant specific heat

$$\begin{aligned} p &= \frac{nRT}{V} \\ e &= c_VT \end{aligned}$$

  with n the quantity of material in $[mol]$, R the gas constant in $[\frac{J}{mol\cdot K}]$ and c_p, c_v the specific heat in $[\frac{J}{kg\cdot K}]$ for a constant pressure and a constant volume respectively.

4.7 Navier-Stokes and Euler equations

Summarising the aforementioned, a system of equations is provided in the well-known Navier-Stokes or Euler form.

4.7.1 Navier-Stokes equations

The system of fluid equations in nonconservation partial differential form, namely (4.5), (4.6) and (4.13):

$$\begin{aligned} \frac{D\rho}{Dt}+\rho\boldsymbol{\nabla}\cdot\boldsymbol{v} &= 0 \\ \rho\boldsymbol{f}-\boldsymbol{\nabla}p+\boldsymbol{\tau}\boldsymbol{\nabla} &= \rho\frac{D\boldsymbol{v}}{Dt} \\ \rho\frac{D}{Dt}\left(e+\frac{v^2}{2}\right) &= \rho\boldsymbol{f}\cdot\boldsymbol{v}+\boldsymbol{\nabla}\cdot(\boldsymbol{\tau}\boldsymbol{v}-\boldsymbol{q}-p\boldsymbol{v}). \end{aligned} \tag{4.25}$$

Together with the Newtonian shear stress equations, Fourier's law and the EOS the dependent variables $\rho, \boldsymbol{v}, e, \rho$ and T can be solved with the independent $x, y, z \in V \wedge t \in [0, \infty)$ with boundary $\partial V = S$ (or Ω with boundary $\partial\Omega = \Gamma$). The system is solvable and thus fully determines the fluid behaviour.

4.7.2 Euler equations

In many cases, when inertia terms due to convective contribution are much bigger then the viscous forces, e.g. in gas dynamics. The viscosity can be neglected and the Navier-Stokes equations become the so-called Euler equations. This is often also referred to as the difference between viscous and inviscid flow. With viscous flow the transport phenomena of friction, mass diffusion and thermal conduction are taken into account. In the inviscid case they are excluded and therefor $\boldsymbol{\tau} = \mathbf{0}$. Herewith, the Euler equations are

$$\begin{aligned} \frac{D\rho}{Dt} + \rho \boldsymbol{\nabla} \cdot \boldsymbol{v} &= 0 \\ \rho \boldsymbol{f} - \boldsymbol{\nabla} p &= \rho \frac{D\boldsymbol{v}}{Dt} \\ \rho \frac{D}{Dt}\left(e + \frac{v^2}{2}\right) &= \rho \boldsymbol{f} \cdot \boldsymbol{v} - \boldsymbol{\nabla} \cdot (\boldsymbol{q} + p\boldsymbol{v}). \end{aligned} \tag{4.26}$$

4.7.3 Initial and boundary conditions

To solve (4.25) uniquely, you need initial and boundary conditions (IC and BC). This is determined by looking at the highest order of derivatives in time and space for each dependent variable. The dependent variables are $\rho, \boldsymbol{v}, e, p$ and $\boldsymbol{q}$.

The highest order of derivatives of ρ are included in $\boldsymbol{\nabla} \cdot (\rho \boldsymbol{v}) = \rho \cdot \boldsymbol{\nabla} \boldsymbol{v} + \boldsymbol{\nabla} \rho \cdot \boldsymbol{v}$. For the case $\boldsymbol{\nabla}\star$ it is known that one BC at the inflow boundary suffices [8]. Thus, one BC at the inflow boundary for ρ is needed. An IC is needed for the term $\frac{\partial \rho}{\partial t}$.

For $\boldsymbol{v}$ the terms $\boldsymbol{(v \cdot \nabla) v}$, $\boldsymbol{\tau v}$ and $\boldsymbol{\nabla \cdot (\tau v)}$ determine what kind of BC is needed. In particular $\boldsymbol{\tau} = \boldsymbol{\tau}(\boldsymbol{v})$. In the Newtonian case as discussed in 4.6.1, $\boldsymbol{\tau} = \boldsymbol{\tau}(\boldsymbol{\nabla} \cdot \boldsymbol{v})$. Herewith, the term $\boldsymbol{\nabla \cdot (\tau v)}$ results in second order derivatives that need a BC for the whole boundary [8]. Again, one IC is needed for $\frac{\partial \boldsymbol{v}}{\partial t}$.

The internal energy e is included in $\frac{\partial e}{\partial t}$, $\boldsymbol{\nabla} e$ and $\boldsymbol{\nabla} \cdot \boldsymbol{q}$. With (4.23), $\boldsymbol{q} = \boldsymbol{q}(T(\rho, e))$ with first order derivatives $\boldsymbol{\nabla}$. Term $\boldsymbol{\nabla} \cdot \boldsymbol{q}$ thus results in the need for a BC for e over the whole boundary. And $\frac{\partial e}{\partial t}$ for one IC.

Variables p and $\boldsymbol{q}$ need not be considered because they are functions of ρ and e and thus the necessary conditions are already provided.

To summarise, for the Navier-Stokes equations in combination with its additional relations the need for ICs and BCs consists of

- ICs for $\rho, \boldsymbol{v}$ and e
- inflow BC for ρ
- BCs for the whole boundary for $\boldsymbol{v}$ and e.

For the Euler equations, the demands are smaller. The terms $\boldsymbol{\tau v}$ and $\boldsymbol{\nabla \cdot (\tau v)}$ are no longer of concern because $\boldsymbol{\tau} = \mathbf{0}$. Hence, only $\boldsymbol{\nabla} \cdot \boldsymbol{v}$ is left, so only a BC a the inflow boundary is needed.

The specific case of ICs and BCs for hydroplaning is treated in 4.8 and 4.9.

4.7.4 Non-dimensionalising the Navier-Stokes equations

Non-dimensionalising a set of equations yields a dimensionless form of the set. Dimension analysis by using the theorem of Buckingham [24] gives insight in the scaling relations of the system without using knowledge about the solutions. A corollary is that the total number of variables and parameters is minimal, making the equations easier in consideration. This minimisation is also the purpose of scaling. These techniques show that it is not useful to vary all the variables and parameters seperately to gain knowledge about the

system, but that only certain combinations of them matter. The scaling used to simplify the Navier-Stokes equations is

$$\bar{\boldsymbol{x}} = \frac{\boldsymbol{x}}{L}, \quad \bar{\boldsymbol{\nabla}} = \frac{\boldsymbol{\nabla}}{\frac{1}{L}}, \quad \bar{t} = \frac{t}{\frac{L}{U}}, \quad \bar{\boldsymbol{v}} = \frac{\boldsymbol{v}}{U}, \quad \bar{\boldsymbol{D}} = \frac{\boldsymbol{D}}{\frac{U}{L}}, \quad \bar{\boldsymbol{f}} = \frac{\boldsymbol{f}}{\frac{U^2}{L}}, \quad \bar{\rho} = \frac{\rho}{\rho_0}, \quad \bar{p} = \frac{p}{\rho_0 U^2} \tag{4.27}$$

with L, U and ρ_0 a characteristic length, speed and density for the system. Note that these characteristics are not determined physically but merely chosen to suit the considered system. Writtin in this way, it is evident that the dimensions of the nominator and denominator of the scaled parameters are equal and thus the parameters itself are dimensionless.

The scaling (4.27) yields for (4.5)

$$\begin{aligned}
\frac{D\rho}{Dt} + \rho\boldsymbol{\nabla}\cdot\boldsymbol{v} = 0 \quad &\Leftrightarrow \quad \frac{D(\rho_0\bar{\rho})}{D(\frac{L}{U}\bar{t})} + \rho_0\bar{\rho}\frac{\bar{\boldsymbol{\nabla}}}{L}\cdot(U\bar{\boldsymbol{v}}) = 0 \\
&\Leftrightarrow \quad \frac{\rho_0 U}{L}\frac{D\bar{\rho}}{D\bar{t}} + \frac{\rho_0 U}{L}\bar{\rho}\bar{\boldsymbol{\nabla}}\cdot\bar{\boldsymbol{v}} = 0 \\
&\Leftrightarrow \quad \frac{D\bar{\rho}}{D\bar{t}} + \bar{\rho}\bar{\boldsymbol{\nabla}}\cdot\bar{\boldsymbol{v}} = 0
\end{aligned}$$

and for (4.6)

$$\begin{aligned}
\rho\frac{D\boldsymbol{v}}{Dt} = \rho\boldsymbol{f} - \boldsymbol{\nabla}p + \boldsymbol{\tau}\boldsymbol{\nabla} \quad &\Leftrightarrow \quad \rho\frac{D\boldsymbol{v}}{Dt} = \rho\boldsymbol{f} - \boldsymbol{\nabla}p + 2\mu\boldsymbol{D}\boldsymbol{\nabla} \\
&\Leftrightarrow \quad \rho_0\bar{\rho}\frac{D(U\bar{\boldsymbol{v}})}{D(\frac{L}{U}\bar{t})} = \rho_0\bar{\rho}\frac{U^2}{L}\bar{\boldsymbol{f}} - \frac{\bar{\boldsymbol{\nabla}}}{L}(\rho_0 U^2\bar{p}) + 2\mu\frac{U}{L}\bar{\boldsymbol{D}}\frac{\bar{\boldsymbol{\nabla}}}{L} \\
&\Leftrightarrow \quad \frac{\rho_0 U^2}{L}\frac{D\bar{\boldsymbol{v}}}{D\bar{t}} = \frac{\rho_0 U^2}{L}\bar{\rho}\bar{\boldsymbol{f}} - \frac{\rho_0 U^2}{L}\bar{\boldsymbol{\nabla}}\bar{p} + \frac{2\mu U}{L^2}\bar{\boldsymbol{D}}\bar{\boldsymbol{\nabla}} \\
&\Leftrightarrow \quad \frac{D\bar{\boldsymbol{v}}}{D\bar{t}} = \bar{\rho}\bar{\boldsymbol{f}} - \bar{\boldsymbol{\nabla}}\bar{p} + 2\frac{\mu}{\rho_0 UL}\bar{\boldsymbol{D}}\bar{\boldsymbol{\nabla}} \\
&\Leftrightarrow \quad \frac{D\bar{\boldsymbol{v}}}{D\bar{t}} = \bar{\rho}\bar{\boldsymbol{f}} - \bar{\boldsymbol{\nabla}}\bar{p} + \frac{2}{Re}\bar{\boldsymbol{D}}\bar{\boldsymbol{\nabla}}
\end{aligned}$$

where Re is the Reynolds number. The Reynolds number represents the ratio between inertial forces ρU and viscous forces $\frac{\mu}{L}$, both in $[\frac{N}{m^3 s}]$, force per volume per second. Consequently, it quantifies the relative importance of these two types of forces. It is the most important dimensionless number in fluid dynamics and is used to provide a criterion for determining dynamic similitude. When two geometrically similar flow patterns, in perhaps different fluids with possibly different flowrates, have the same values for the relevant dimensionless numbers, they are said to be dynamically similar, and will have similar flow geometry.

The Reynolds number is also used to identify and predict different flow regimes, such as laminar or turbulent flow. Laminar flow occurs at low Reynolds numbers, where viscous forces are dominant, and is characterized by smooth, constant fluid motion. Turbulent flow, on the other hand, occurs at high Reynolds numbers and is dominated by inertial forces, which tend to produce vortices and other flow fluctuations.

$$\begin{aligned}
Re &= \frac{\text{dynamic pressure}}{\text{shearing stress}} = \frac{\frac{\rho_0 U^2}{L}}{\frac{\mu U}{L^2}} \\
&= \frac{\text{inertia forces}}{\text{viscous forces}} = \frac{\rho_0 U}{\frac{\mu}{L}} \\
&= \frac{\rho_0 UL}{\mu}
\end{aligned}$$

We skip the scaling of (4.13) because it is not of interest in the case of hydroplaning. Argumentation for this can be found in 4.8.4.

Non-dimensionalising the ICs and BCs goes in a similar way.

4.8 Hydroplaning case

Concerning the case of hydroplaning, some assumptions can be made for the fluid equations. The fluid is considered to be incompressible, isotropic and Newtonian viscous with a constant viscosity μ. Furthermore, the only body force that is present is gravitation.

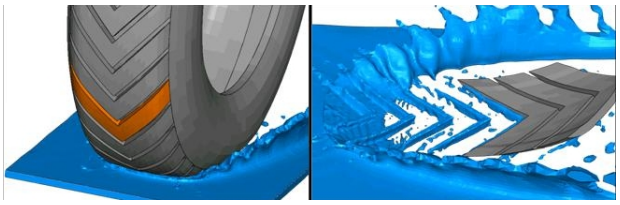

Figure 4.6: incompressible, viscous flow.

4.8.1 Incompressibility and isotropy

In an incompressible flow, the volume is unchanged during deformation and the density ρ remains constant. A motion of an incompressible material is called isochoric. Thus, in formula, incompressibility means

$$J = \det(\boldsymbol{F}) = 1,\ \rho = \text{constant and } e = cT \tag{4.28}$$

where J is called the Jacobian and $\boldsymbol{F} = \frac{\partial \boldsymbol{x}}{\partial \boldsymbol{X}}$ the deformation gradient with $\boldsymbol{X}$ the material particle points and $\boldsymbol{x}$ the spatial particle points, not to be confused with independent variables x, y, z. In other words, particles of a body described by coordinates $\boldsymbol{X}$ are strained to new body coordinates $\boldsymbol{x}$ [5]. Furthermore [2], Poisson's ratio $\nu = \frac{1}{2} \Leftrightarrow K = \infty$ with K the bulk modulus. These quantities will also be used later on in 5.4.2. It is often useful, particularly for incompressible materials, to write the stress and strain rate measures as the sum of deviatoric and hydrostatic or volumetric parts. The latter is also called the spherical part of a tensor. Conditions (4.28) imply that $\frac{D\rho}{Dt} = 0$. As a consequence, (4.5) becomes

$$\rho \boldsymbol{\nabla} \cdot \boldsymbol{v} = 0.$$

Note that because $\rho = \text{constant} \neq 0$

$$\boldsymbol{\nabla} \cdot \boldsymbol{v} = 0$$

holds. We say that the velocity is solenoidal or divergence free.

Isotropy of the fluid implies that the coefficient of thermal conductivity k is independent of the spacial coordinates and thus a constant.

The solenoidal velocity and isotropy in combination with (4.23) simplifies the energy equation (4.13) to

$$\rho \frac{D}{Dt}\left(cT + \frac{v^2}{2}\right) = \rho \boldsymbol{f} \cdot \boldsymbol{v} + \boldsymbol{\nabla} \cdot (\boldsymbol{\tau} \boldsymbol{v} + k \boldsymbol{\nabla} T).$$

4.8.2 Newtonian viscous flow

From the assumption that the flow is Newtonian viscous it follows that the shear stresses suffice to the relations described in 4.6.1. Together with the incompressibility condition $\boldsymbol{\nabla} \cdot \boldsymbol{v} = 0$ the shear stresses become

$$\tau_{xx} = \sigma_x = 2\mu \frac{\partial u}{\partial x} \tag{4.29}$$

$$\tau_{yy} = \sigma_y = 2\mu \frac{\partial v}{\partial y} \tag{4.30}$$

$$\tau_{zz} = \sigma_z = 2\mu \frac{\partial w}{\partial z} \tag{4.31}$$

$$\tau_{xy} = \tau_{yx} = \mu\left(\frac{\partial v}{\partial x} + \frac{\partial u}{\partial y}\right) \tag{4.32}$$

$$\tau_{xz} = \tau_{zx} = \mu\left(\frac{\partial u}{\partial z} + \frac{\partial w}{\partial x}\right) \tag{4.33}$$

$$\tau_{yz} = \tau_{zy} = \mu\left(\frac{\partial w}{\partial y} + \frac{\partial v}{\partial z}\right). \tag{4.34}$$

In this way, we get

$$\boldsymbol{\tau} \boldsymbol{\nabla} = \mu \begin{pmatrix} 2\frac{\partial^2 u}{\partial x^2} + \frac{\partial^2 v}{\partial x \partial y} + \frac{\partial^2 u}{\partial y^2} + \frac{\partial^2 u}{\partial z^2} + \frac{\partial^2 w}{\partial x \partial z} \\ \frac{\partial^2 v}{\partial x^2} + \frac{\partial^2 u}{\partial x \partial y} + 2\frac{\partial^2 v}{\partial y^2} + \frac{\partial^2 w}{\partial y \partial z} + \frac{\partial^2 v}{\partial z^2} \\ \frac{\partial^2 u}{\partial x \partial z} + \frac{\partial^2 w}{\partial x^2} + \frac{\partial^2 w}{\partial y^2} + \frac{\partial^2 v}{\partial y \partial z} + 2\frac{\partial^2 w}{\partial z^2} \end{pmatrix}$$

Furthermore, from $\boldsymbol{\nabla} \cdot \boldsymbol{v} = 0$ it follows that

$$\begin{aligned}
\boldsymbol{\nabla} \cdot \boldsymbol{v} = 0 \quad &\Leftrightarrow \quad \frac{\partial u}{\partial x} + \frac{\partial v}{\partial y} + \frac{\partial w}{\partial z} = 0 \\
&\Leftrightarrow \quad \frac{\partial u}{\partial x} = -\frac{\partial v}{\partial y} - \frac{\partial w}{\partial z} \\
&\Leftrightarrow \quad \frac{\partial^2 u}{\partial x^2} = -\frac{\partial^2 v}{\partial x \partial y} - \frac{\partial^2 w}{\partial x \partial z} \\
&\Leftrightarrow \quad 2\frac{\partial^2 u}{\partial x^2} = \frac{\partial^2 u}{\partial x^2} - \frac{\partial^2 v}{\partial x \partial y} - \frac{\partial^2 w}{\partial x \partial z} \\
&\Leftrightarrow \quad 2\mu\frac{\partial^2 u}{\partial x^2} = \mu\left(\frac{\partial^2 u}{\partial x^2} - \frac{\partial^2 v}{\partial x \partial y} - \frac{\partial^2 w}{\partial x \partial z}\right)
\end{aligned}$$

so that the first row-element of $\boldsymbol{\tau}\boldsymbol{\nabla}$ becomes

$$\begin{aligned}
\mu\left(2\frac{\partial^2 u}{\partial x^2} + \frac{\partial^2 v}{\partial x \partial y} + \frac{\partial^2 u}{\partial y^2} + \frac{\partial^2 u}{\partial z^2} + \frac{\partial^2 w}{\partial x \partial z}\right) &= 2\mu\frac{\partial^2 u}{\partial x^2} + \mu\left(\frac{\partial^2 v}{\partial x \partial y} + \frac{\partial^2 u}{\partial y^2} + \frac{\partial^2 u}{\partial z^2} + \frac{\partial^2 w}{\partial x \partial z}\right) \\
&= \mu\left(\frac{\partial^2 u}{\partial x^2} - \frac{\partial^2 v}{\partial x \partial y} - \frac{\partial^2 w}{\partial x \partial z}\right) + \mu\left(\frac{\partial^2 v}{\partial x \partial y} + \frac{\partial^2 u}{\partial y^2} + \frac{\partial^2 u}{\partial z^2} + \frac{\partial^2 w}{\partial x \partial z}\right) \\
&= \mu\left(\frac{\partial^2 u}{\partial x^2} + \frac{\partial^2 u}{\partial y^2} + \frac{\partial^2 u}{\partial z^2}\right) \\
&= \mu\boldsymbol{\nabla} \cdot \boldsymbol{\nabla} u
\end{aligned}$$

or in short $\boldsymbol{\nabla}^2 u$. In a similar way

$$\begin{aligned}
\frac{\partial^2 v}{\partial x^2} + \frac{\partial^2 u}{\partial x \partial y} + 2\frac{\partial^2 v}{\partial y^2} + \frac{\partial^2 w}{\partial y \partial z} + \frac{\partial^2 v}{\partial z^2} &= \mu\boldsymbol{\nabla}^2 v \\
\frac{\partial^2 u}{\partial x \partial z} + \frac{\partial^2 w}{\partial x^2} + \frac{\partial^2 w}{\partial y^2} + \frac{\partial^2 v}{\partial y \partial z} + 2\frac{\partial^2 w}{\partial z^2} &= \mu\boldsymbol{\nabla}^2 w
\end{aligned}$$

and thus

$$\boldsymbol{\tau}\boldsymbol{\nabla} = \mu\boldsymbol{\nabla}^2\boldsymbol{v}$$

so the momentum equation (4.6) simplifies to

$$\rho\frac{D\boldsymbol{v}}{Dt} = \rho\boldsymbol{f} - \boldsymbol{\nabla}p + \mu\boldsymbol{\nabla}^2\boldsymbol{v}. \tag{4.35}$$

Note that sometimes the scalar operator $\boldsymbol{\nabla} \cdot \boldsymbol{\nabla} = \boldsymbol{\nabla}^2$ is denoted by $\boldsymbol{\Delta}$.

4.8.3 Body force

The only body force present when considering hydroplaning is gravitation which works in the z-direction. Herewith

$$\boldsymbol{f} = \begin{pmatrix} 0 \\ 0 \\ f_z \end{pmatrix} = \begin{pmatrix} 0 \\ 0 \\ g \end{pmatrix} \tag{4.36}$$

with $g = 9.81[\frac{N}{kg}]$ the gravitation-constant.

4.8.4 Decoupled energy equation

The energy equation simplified by the incompressibility condition

$$\rho\frac{D}{Dt}\left(cT + \frac{v^2}{2}\right) = \rho\boldsymbol{f} \cdot \boldsymbol{v} + \boldsymbol{\nabla} \cdot (\boldsymbol{\tau}\boldsymbol{v} - k\boldsymbol{\nabla}T)$$

contains the term $\boldsymbol{\nabla} \cdot \boldsymbol{\tau}\boldsymbol{v}$. With symmetry of the stress matrix $\boldsymbol{\tau} = \boldsymbol{\tau}^T$ we get

$$\begin{aligned}
\boldsymbol{\nabla} \cdot \boldsymbol{\tau}\boldsymbol{v} &= \boldsymbol{\nabla}^T\boldsymbol{\tau}\boldsymbol{v} \\
&= \boldsymbol{\nabla}^T\boldsymbol{\tau}^T\boldsymbol{v} \\
&= (\boldsymbol{\tau}\boldsymbol{\nabla})^T\boldsymbol{v} \\
&= (\mu\boldsymbol{\nabla}^2\boldsymbol{v})^T\boldsymbol{v} \\
&= \mu(\boldsymbol{\nabla}^2\boldsymbol{v})^T\boldsymbol{v} \\
&= \mu\boldsymbol{\nabla}^2\boldsymbol{v} \cdot \boldsymbol{v}
\end{aligned}$$

With the assumptions for the consideration of hydroplaning, the system of equations is now

$$\begin{aligned} \boldsymbol{\nabla} \cdot \boldsymbol{v} &= 0 \\ \rho \frac{D\boldsymbol{v}}{Dt} &= \rho \boldsymbol{f} - \boldsymbol{\nabla} p + \mu \boldsymbol{\nabla}^2 \boldsymbol{v} \\ \rho \frac{D}{Dt}\left(cT + \frac{v^2}{2}\right) &= (\rho \boldsymbol{f} + \mu \boldsymbol{\nabla}^2 \boldsymbol{v}) \cdot \boldsymbol{v} + k \boldsymbol{\nabla}^2 T. \end{aligned} \tag{4.37}$$

Note that the energy equation has been decoupled from the continuity and momentum equations. The last are four equations with four unknowns and can thus be solved on their own. If the problem were to involve heat transfer and hence temperature gradients in the flow, the temperature field is obtained from the energy equation by simply filling in the p and $\boldsymbol{v}$ after. In this case even only $\boldsymbol{v}$ because due to the incompressibility condition $\boldsymbol{\nabla} \cdot \boldsymbol{v} = 0$ the term $\boldsymbol{\nabla} \cdot p\boldsymbol{v} = 0$ in (4.13) and is thus cancelled out.

In the case of hydroplaning we are not interested in the temperature of the fluid and its influence on the tire. Consequently, a review of the energy equation to solve T and the hereby needed EOS are redundant.

4.8.5 Initial and boundary conditions

To solve

$$\begin{aligned} \boldsymbol{\nabla} \cdot \boldsymbol{v} &= 0 \\ \rho \frac{D\boldsymbol{v}}{Dt} &= \rho \boldsymbol{f} - \boldsymbol{\nabla} p + \mu \boldsymbol{\nabla}^2 \boldsymbol{v} \end{aligned} \tag{4.38}$$

uniquely you need initial and boundary conditions. This is determined by looking at the highest order of derivatives in time and space for each dependent variable. Where in the compressible case $p = p(e, \rho)$, in the incompressible case we have $\rho =$ constant and a decoupled energy equation cf. 4.8.4 whereby p becomes a focal variable itself. So the dependent variables are p and $\boldsymbol{v}$.

The highest order of derivatives of p are included in $\boldsymbol{\nabla} p = \begin{pmatrix} \frac{\partial p}{\partial x} & \frac{\partial p}{\partial y} & \frac{\partial p}{\partial z} \end{pmatrix}^T$. For the case $\boldsymbol{\nabla} \star$ it is known that one BC at the inflow boundary suffices [8]. However, this BC is already 'concealed' in the constraint $\boldsymbol{\nabla} \cdot \boldsymbol{v} = 0$ in (4.38). At first sight this is hard to see. Applying $\boldsymbol{\nabla} \cdot$ to (4.38) however, yields

$$\begin{aligned} \boldsymbol{\nabla} \cdot \left(\rho \frac{D\boldsymbol{v}}{Dt}\right) &= \boldsymbol{\nabla} \cdot \left(\rho \boldsymbol{f} - \boldsymbol{\nabla} p + \mu \boldsymbol{\nabla}^2 \boldsymbol{v}\right) \\ \boldsymbol{\nabla} \cdot \rho \frac{D\boldsymbol{v}}{Dt} &= \boldsymbol{\nabla} \cdot \rho \boldsymbol{f} - \boldsymbol{\nabla} \cdot \boldsymbol{\nabla} p + \boldsymbol{\nabla} \cdot \mu \boldsymbol{\nabla}^2 \boldsymbol{v} \\ \rho \frac{D(\boldsymbol{\nabla} \cdot \boldsymbol{v})}{Dt} &= \rho \boldsymbol{\nabla} \cdot \boldsymbol{f} - \boldsymbol{\nabla}^2 p + \mu \boldsymbol{\nabla}^2 (\boldsymbol{\nabla} \cdot \boldsymbol{v}) \\ 0 &= \rho \boldsymbol{\nabla} \cdot \boldsymbol{f} - \boldsymbol{\nabla}^2 p \\ \boldsymbol{\nabla}^2 p &= \rho \boldsymbol{\nabla} \cdot \boldsymbol{f}, \end{aligned} \tag{4.39}$$

a Poisson equation for p. Herewith, a BC is already provided. There is no time derivative of the pressure present so in no IC is needed.

The highest order of derivatives in space and time of $\boldsymbol{v}$ are included in $\boldsymbol{\nabla}^2 \boldsymbol{v}$ and $\frac{D\boldsymbol{v}}{Dt}$ respectively. Accordingly, a BC at the whole boundary and one IC are needed [8].

To summarise, for the incompressible, Newtonian viscous Navier-Stokes equations the need for ICs and BCs consists of

- IC for $\boldsymbol{v}$
- BC for the whole boundary for $\boldsymbol{v}$.

The IC for the velocity is $\boldsymbol{v} = \boldsymbol{0}$, because the puddle is assumed non-moving on the tarmac.
The fluid is in contact with either the air, the tarmac or the tire. Everywhere along the boundary the velocity $\boldsymbol{v}$ should be pescribed. Where the fluid is in contact with air, the velocity follows from $\boldsymbol{\tau}(\boldsymbol{v}) = \boldsymbol{0}$, because the stresses coming from the air are negligable. The tarmac and tire have velocities $\boldsymbol{v} = \boldsymbol{0}$ and $\boldsymbol{v} = \boldsymbol{\omega} \times \boldsymbol{r}$ respectively with $\boldsymbol{\omega}$ and $\boldsymbol{r}$ the rotational speed in $[\frac{rad}{s}]$ and radius of the tire in $[m]$. As a result of adhesion the velocity of the fluid equals the velocity of the tarmac and tire at the designated boundaries. These are also called no slip conditions.

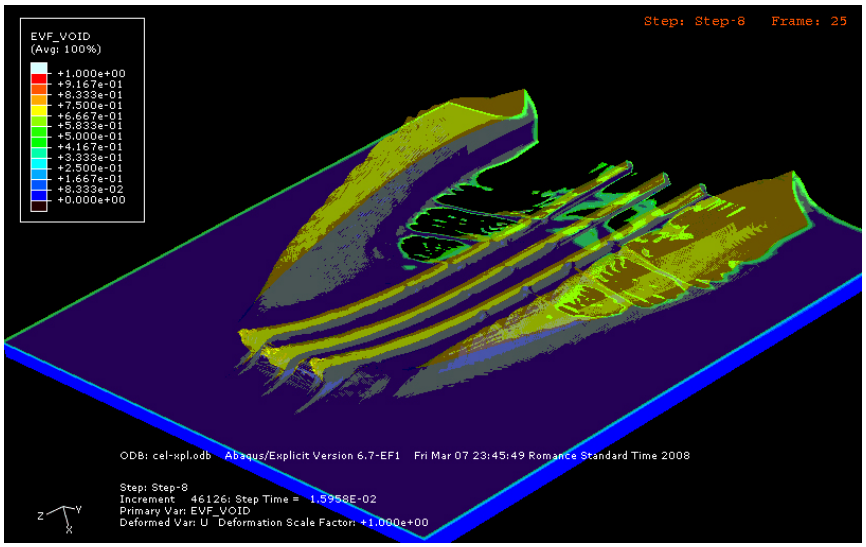

Figure 4.7: simulation of fluid flow with hydroplaning. Fluid is in contact with either the air, the tarmac or the tire.

4.8.6 Non-dimensionalising the incompressible Navier-Stokes equations

The non-dimensionalising of the incompressible Navier-Stokes equations is similar to the compressible case.

$$\bar{\boldsymbol{x}} = \frac{\boldsymbol{x}}{L}, \quad \bar{\boldsymbol{\nabla}} = \frac{\boldsymbol{\nabla}}{\frac{1}{L}}, \quad \bar{t} = \frac{t}{\frac{L}{U}}, \quad \bar{\boldsymbol{v}} = \frac{\boldsymbol{v}}{U}, \quad \bar{\boldsymbol{f}} = \frac{\boldsymbol{f}}{\frac{U^2}{L}}, \quad \bar{\rho} = \frac{\rho}{\rho_0}, \quad \bar{p} = \frac{p}{\rho_0 U^2} \tag{4.40}$$

with L, U and ρ_0 a characteristic length, speed and density for the system. As characteristic length we choose the width of the tire $L = 0.220[m]$. For characteristic speed the speed where hydroplaning starts occuring would be appropriate, so $U \in [80, 100][\frac{km}{h}]$. We assumed incompressibility so $\rho =$ constant. Choose the density of water, namely $\rho_0 = 1000[\frac{kg}{m^3}]$.

The scaling (4.40) yields for (4.37)

$$\begin{aligned} \boldsymbol{\nabla} \cdot \boldsymbol{v} = 0 \quad &\Leftrightarrow \quad \frac{\bar{\boldsymbol{\nabla}}}{L} \cdot (U\bar{\boldsymbol{v}}) = 0 \\ &\Leftrightarrow \quad \frac{U}{L}\bar{\boldsymbol{\nabla}} \cdot \bar{\boldsymbol{v}} = 0 \\ &\Leftrightarrow \quad \bar{\boldsymbol{\nabla}} \cdot \bar{\boldsymbol{v}} = 0 \end{aligned}$$

and

$$\begin{aligned} \rho\frac{D\boldsymbol{v}}{Dt} = \rho\boldsymbol{f} - \boldsymbol{\nabla}p + \mu\boldsymbol{\nabla}^2\boldsymbol{v} \quad &\Leftrightarrow \quad \rho_0\bar{\rho}\frac{D(U\bar{\boldsymbol{v}})}{D(\frac{L}{U}\bar{t})} = \rho_0\bar{\rho}\frac{U^2}{L}\bar{\boldsymbol{f}} - \frac{\bar{\boldsymbol{\nabla}}}{L}(\rho_0 U^2\bar{p}) + \mu\left(\frac{\bar{\boldsymbol{\nabla}}}{L}\right)^2 U\bar{\boldsymbol{v}} \\ &\Leftrightarrow \quad \frac{\rho_0 U^2}{L}\bar{\rho}\frac{D\bar{\boldsymbol{v}}}{D\bar{t}} = \frac{\rho_0 U^2}{L}\bar{\rho}\bar{\boldsymbol{f}} - \frac{\rho_0 U^2}{L}\bar{\boldsymbol{\nabla}}\bar{p} + \frac{\mu U}{L^2}\bar{\boldsymbol{\nabla}}^2\bar{\boldsymbol{v}} \\ &\Leftrightarrow \quad \bar{\rho}\frac{D\bar{\boldsymbol{v}}}{D\bar{t}} = \bar{\rho}\bar{\boldsymbol{f}} - \bar{\boldsymbol{\nabla}}\bar{p} + \frac{\mu}{\rho_0 UL}\bar{\boldsymbol{\nabla}}^2\bar{\boldsymbol{v}} \\ &\Leftrightarrow \quad \bar{\rho}\frac{D\bar{\boldsymbol{v}}}{D\bar{t}} = \bar{\rho}\bar{\boldsymbol{f}} - \bar{\boldsymbol{\nabla}}\bar{p} + \frac{1}{Re}\bar{\boldsymbol{\nabla}}^2\bar{\boldsymbol{v}}. \end{aligned}$$

Herewith, and noting that $\mu_{\text{water}} = 8.90 \cdot 10^{-4}[Pa \cdot s]$, the Reynolds number is $Re = \frac{\rho_0 UL}{\mu} = \frac{1000\frac{U}{3.6}0.220}{8.90 \cdot 10^{-4}} \in [5.49 \cdot 10^6, 6.87 \cdot 10^6] = O(10^6)$.

Non-dimensionalising the ICs and BCs goes in a similar way.

4.9 Abaqus case

As of this time, this section is still in an early fase. Progress is made during the Master project to obtain background information about the methods used in solving FSI problems like hydroplaning using Abaqus'

CEL method. There are some facts that we do know at the moment [21, 22].

4.9.1 Obscurities

Unaccordingly with 4.8, Abaqus uses the compressible form of the fluid equations. In combination with a high bulk modulus K, the incompressible case is approximated. The infamous problems arising with the incompressible form, e.g. singularities in the system of equations, are however not circumvented in this way. The higher the bulk modulus, the more these problems show up. Methods like the penalty function method and alternative geometric locations of the variables within the discretisation elements are used to solve these issues.

How the energy equation fits within this frame is unclear. In the compressible case it is mandatory to solve it, whilst approaching the incompressible case its importance decreases. The usage of EOS for material properties is a fact however, see 4.9.2, which states the relations $p = p(e, \rho)$ and $T = T(e, \rho)$.

The fluid equations are solved explicitely [22]. This implies that no implicit iterations are made to solve the nonlinear term. One or both of the factors in the nonlinear term $(\boldsymbol{v} \cdot \boldsymbol{\nabla})\boldsymbol{v}$ is apparently taken at the previous timestep to linearise it.

The elements used in the finite element formulation of the problem are EC3D8R, which stands for Eulerian (E), continuum (C), three-dimensional (3D) elements with a reduced amount of integration points (R). In case of a structure, this reduction calls in the need for hourglass stiffness control to solve the issue of singularities in the system. Unexpectedly, this is not used in the case of fluids. It can be concluded that the singularities are treated in an other way. Which, is unknown at this time.

The basis functions are linear. This option is fixed. This is contradicting the typically taking the order of p one lower than of $\boldsymbol{v}$. The geometric locations of the variables within the elements are unknown. Simulia, however, does not exactly shun extrapolation in this case.

It is stated that the momentum equation for the fluid is solved in the same way as for the structure [22], namely solving $\rho\frac{\partial^2 x}{\partial t^2} = \boldsymbol{\tau}\boldsymbol{\nabla}$ instead of $\rho\frac{\partial v}{\partial t} = \boldsymbol{\tau}\boldsymbol{\nabla}$. This approach we have never heard of. Neither have colleagues at the universities. Clarification is to follow.

This lack of information yields the postponement of stating details of the weak formulation and usage of FEM.

4.9.2 Mie-Grüneisen with Hugoniot fit

The EOS used by Abaqus is Mie-Grüneisen with a Hugoniot fit.

The most common form of Mie-Grüneisen is

$$p - p_H = \Gamma\rho(e - E_H), \tag{4.41}$$

where p_H and E_H are the Hugoniot pressure and specific energy per unit mass and are functions of density only. The Hugoniot pressure p_H is, in general, defined from experimental data (curve-fitting). The Γ is the Grüneisen ratio which describes the alteration in a crystal lattice's vibration's frequency, also called a phonon, based on the lattice's increase or decrease in volume as a result of temperature change. It is used in quantummechanics and is defined as

$$\Gamma = \Gamma_0\frac{\rho_0}{\rho} \tag{4.42}$$

where Γ_0 is the initial Grüneisen ratio and ρ_0 is the reference density. The Hugoniot energy E_H is related to p_H by

$$E_H = \frac{p_H\eta}{2\rho_0} \tag{4.43}$$

where $\eta = 1 - \frac{\rho_0}{\rho}$ is the nominal volumetric compressive strain. Elimination of Γ and E_H from (4.41) yields

$$p = p_H\left(1 - \frac{\Gamma_0\eta}{2}\right) + \Gamma_0\rho_0 e. \tag{4.44}$$

The EOS and the energy equation represent coupled equations for pressure and internal energy. Abaqus/Explicit, the solver of Abaqus using explicit methods only, solves these equations simultaneously at each material point.

A common fit to the Hugoniot data is given by

$$p_H = \frac{\rho_0 c_0^2 \eta}{(1 - s\eta)^2} \tag{4.45}$$

where c_0 and s define the linear relationship between the shock velocity U_s and the particle velocity U_p , both in $[\frac{m}{s}]$, as follows:

$$U_s = c_0 + sU_p.$$

With these assumptions (4.44) becomes

$$p = \frac{\rho_0 c_0^2 \eta}{(1 - s\eta)^2} \left(1 - \frac{\Gamma_0 \eta}{2}\right) + \Gamma_0 \rho_0 e \tag{4.46}$$

where $\rho_0 c_0^2 > 0$ is equivalent to the elastic bulk modulus at small nominal strains.

In the case of modelling water, Abaqus prescribes $s = 0 \wedge \Gamma_0 = 0$. Filling this in leads to an simplifaction of the EOS:

$$p|_{s=0 \wedge \Gamma_0 = 0} = \left[\frac{\rho_0 c_0^2 \eta}{(1 - s\eta)^2} \left(1 - \frac{\Gamma_0 \eta}{2}\right) + \Gamma_0 \rho_0 e \right]_{s=0 \wedge \Gamma_0 = 0} = \rho_0 c_0^2 \eta.$$

Recalling that $\eta = 1 - \frac{\rho_0}{\rho}$ we get

$$p = \rho_0 c_0^2 (1 - \frac{\rho_0}{\rho}).$$

Note that by definition of the physical quantities pressure and density it holds that $0 < p, \rho < \infty$. From $p > 0$ it follows that

$$\rho_0 c_0^2 (1 - \frac{\rho_0}{\rho}) > 0 \quad \Rightarrow_{\rho_0 c_0^2 > 0} \quad 1 - \frac{\rho_0}{\rho} > 0 \quad \Leftrightarrow \quad 1 > \frac{\rho_0}{\rho} \quad \Leftrightarrow_{\rho > 0} \quad \rho > \rho_0$$

so $0 < p < \infty \wedge 0 < \rho_0 \leq \rho < \infty$. Herewith

$$\lim_{\rho \to \rho_0} p = 0 \wedge \lim_{\rho \to \infty} p = \rho_0 c_0^2.$$

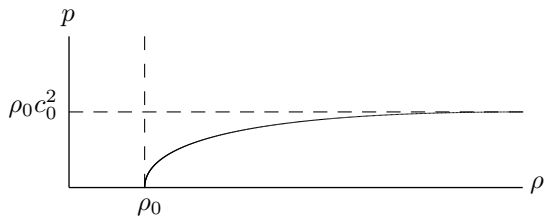

Figure 4.8: relation between pressure p and density ρ.

The Mie-Grüneisen EOS are normally used when considering processes with high pressures and high sound-velocities, e.g. SONAR or explosive applications. Therefor, at first hand the choice seems unlogical. Filling in $s = 0 \wedge \Gamma_0 = 0$ simplifies the relation between pressure p and density ρ to a simple inversely proportional equation. Claim is that this simplification suffices for the modelling of water. The reasoning is that water is nearly incompressibel and therefor the relation between p and ρ is linear in the neighbourhood of ρ_0, cf. Figure 4.8. Nevertheless, Simulia can not explain why their Mie-Grüneisen model differs from references, e.g. [7, 15].

Chapter 5

The tire

5.1 Introduction

Although a tire seems to be a simple torus of rubber, it is more than that. A tire is composed of different materials which assembled must suffice to certain demands. It is the only interface between the vehicle/driver and the road.

So what is a tire?

- Geometrically: a torus.
- Mechanically: a flexible membrane pressure container.
- Structurally: a high performance composite.
- Chemically: compostion of long-chain macromolecules.

This chapter aims to describe the components of a tire and their functions.

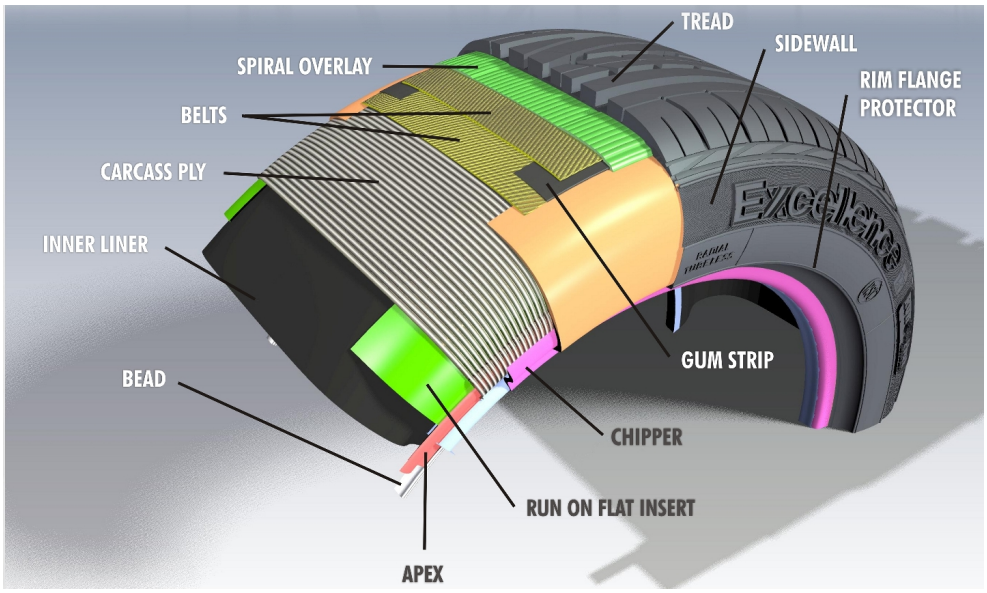

Figure 5.1: tire components.

5.2 Functions and components

What are the demands for a tire? The principal functions of a tire are load carrying capacity, geometric stability, damping vibrations (mechanical and acoustic), transmission of acceleration forces in longitudinal and lateral directions, steering response, good mileage, low fuel consumption, and safety. Some of these functions can be realized by just the application of rubber, but to improve the perfromance, reinforcing agents must be added. The design must be a compromise of the many factors that come into play. In the majority of applications, the tire is to operate on a variety of road surfaces in different weather conditions with a performance as uniform as possible.

In this section the components a tire consists of are explained (Figures 5.1, 5.2 and 5.3). The components can be sorted in three groups: tread, carcass and belt package.

5.2.1 Carcass

The carcass consists of high elastic modulus cords (e.g. steel, nylon, rayon, Kevlar) and low elastic modulus elastomeric compounds.

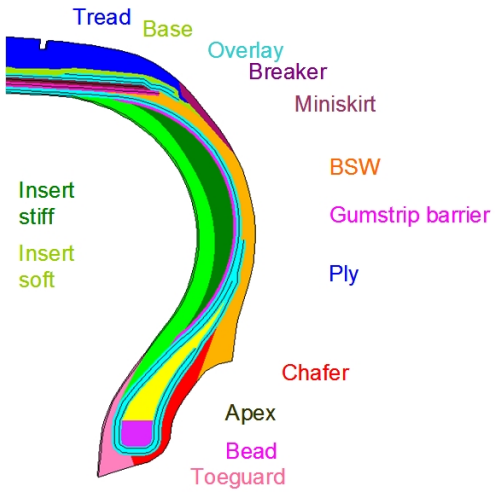

Figure 5.2: tire cross-section.

- **Ply** is made of multiple flexible high elastic modulus cords embedded and bonded to a matrix of low elastic modulus elastomeric material. The number of the layers depends on the tire type, the tire size, the inflation pressure and the speed rating. Its function is to give basic shape to the tire.
- **Liner** is the first tire component that faces the inflation pressure. It stops or reduces air diffusion and keeps the inflation pressure constant during service.
- **Bead** is a ring-like structural component which carries the load generated in the ply cords due to inflation. It is the component that holds the tire locked against the rim under different loading conditions.
- **Apex** is a polymeric component placed in the bead area, i.e. in the lower sidewall. It has three primary functions: to act as filler, to provide the desirable gauge between the ply and the ply turn-up, to increase the stiffness of the lower sidewall and to reduce the lateral tire displacement and to define the ply-line in the lower sidewall region for a given mold shape.
- **Toeguard** is a polymeric component which reduces the possibility of tire damage during mounting and dismounting.
- **Chipper** increases the stiffness of the lower sidewall and increases lateral stiffness.
- **Black SideWall** has several functions. It defines ply-line for given mold shape, defines stiffness distribution along ply, protects the ply by providing scuff resistance and influences damping characteristics of the tire.
- **Chafer** has the following functions: to provide proper interface between tire and rim for good fitment which reduces tire-rim slip and maintains inflation pressure, to reduce/eliminate bead area chafing during service.
- **Soft and stiff inserts** are only present in 'run-on-flat' tires. When a tire is punctured and deflates because of this, the soft and stiff inserts are the backup for driving to the nearest garage.

5.2.2 Belt package

The belt package conists of usually two belts of reinforcement cords lying between the carcass and tread. Its function is to control tire growth during inflation, provide rigidity to the tread to prevent distortions in the lateral direction during manoeuvres, reduce tread wear, give lateral and torsional stiffness to improve handling, supply puncture resistance and protect carcass from failure. It consists of the following components.

- **Belts** are made up of flexible high elasticity modulus cords bonded to a matrix of low elasticity modulus material.
- **Overlay** is a rubber-coated fabric cord layer. Its aim is to reduce tire deformations at high speed. The cords are usually in nylon and are circumferentially oriented.
- **Shoulder wedge** is the upper portion of the sidewall just below the tread edge. Shoulder design affects temperature development in the belt edges and cornering characteristics.

5.2.3 Tread

The tread is the component in contact with the road. It ensures that all driving forces are properly transmitted via a Coulomb friction mechanism under a broad range of environmental conditions. It has to be designed for wear-out resistance, traction, silent running and low heat build-up. The composition of the rubber, the cross-sectional shape of the tread, the number of ribs and grooves are important to determine wear, traction and running temperature perfomance.

- **Ribs** are the circumferential rows of tread rubber in direct contact with the road surface.
- **Grooves** are the channels between the tread ribs and are essential for traction, resistance to aquaplaning, directional control and cool-running properties. Treadwear indicators are molded into the bottom of the tread grooves to indicate when the tire should be replaced.
- **Tread base** is placed between the tread cap and the belt package in some tire constructions to improve energy efficiency or to reduce the operating temperature of the crown area.

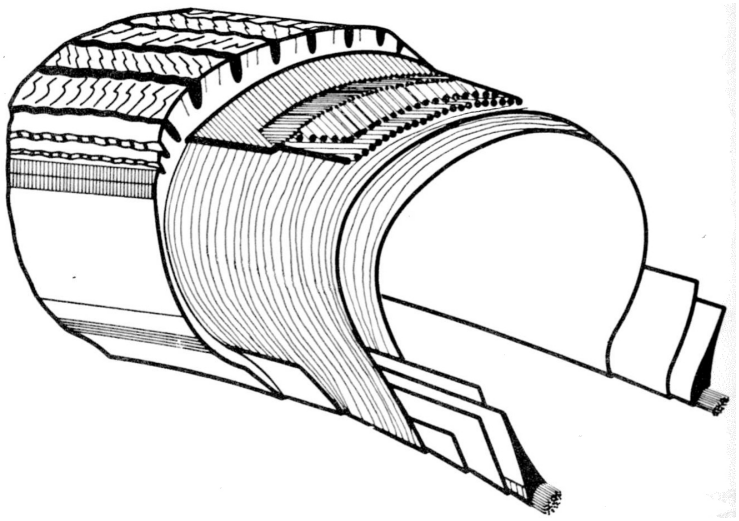

Figure 5.3: tire components [23].

5.3 Materials

The materials to be used in tires must deal with a lot of contradicting demands. A tire needs to have grip. Grip increases with the temperature, but so does indurability. A winter-tire should have grip at low temperatures, but not be frictionless at high temperatures. Periodicity of the treadprofile makes the adhesion uniform and thus comfortable, but also comes with resonance resulting in sound. These contradictions make the task to find a proper material harder.

Besides that, governments prescribe regulations for tires. Certain solvents used in the past for producing tires have been forbidden due to the health of personal in tire plants. Tires have to suffice to criteria like durability, maximum speed and maximum load. Mentioning these criteria on the tire itself is obligatory.

Rubber can be produced in a way that a compromise is possible. This compromise is made by the use of fillers and vulcanization chemicals.

Fillers are added to the compound to improve hardness, stiffness and abrasion resistance. Hereby the size, amount and dispersion of the particles of the fillers is of importance. The traditional filler is carbon black.

Vulcanization chemicals include the initiators, accelerators and sulphur. During vulcanization, rubber molecules are cross-linked by atoms of sulphur. This makes the material harder, more durable and more resistant to chemical attacks. The surface of the material gets smoother and prevents it from sticking to metal or plastic chemical catalysts.

Rubber is a viscoelastic material. Viscoelasticity is the property of materials that exhibit both viscous and elastic characteristics when undergoing deformation. A viscoelastic material has the following properties:

- hysteresis is seen in the stress-strain curve: history dependent behaviour between stress and strain
- stress relaxation occurs: step constant strain causes decreasing stress
- creep occurs: step constant stress causes increasing strain.

Viscoelastic behavior is comprised of elastic and viscous components modeled as linear combinations of springs and dashpots, respectively. Each model differs in the arrangement of these elements. The elastic components, as previously mentioned, can be modeled as springs of elastic constant E, given the formula:

$$\sigma = E\epsilon$$

where σ is the normal stress in $[Pa]$, E is the elastic modulus of the material in $[Pa]$ and ϵ is the strain that occurs under the given stress, conform Hooke's Law [19]. The viscous components can be modeled as dashpots such that the stress-strain rate relationship can be given as

$$\sigma = \mu \frac{d\epsilon}{dt}$$

where μ is viscosity in $[Pa \cdot s]$ and t the time in $[s]$. Famous models that arrange these elements are the Maxwell, Kelvin-Voigt and Standard Linear Solid models (Figures 5.4, 5.5 and 5.6 respectively).

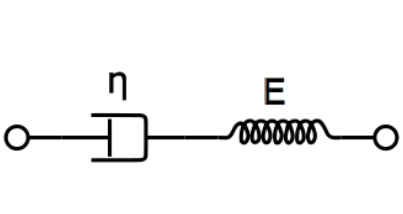

Figure 5.4: Maxwell model.

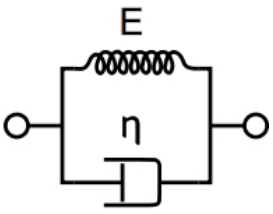

Figure 5.5: Kelvin-Voigt model.

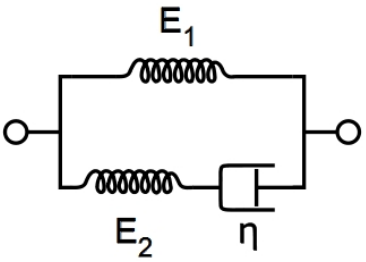

Figure 5.6: Standard Linear Solid model.

The springs and dashpots in these models determine the loss modulus G'' and storage modulus G' respectively, cf. Figure 5.7. An explanation hereof belongs in the discipline material science and is thus beyond the scope of this report. These moduli are related to the material model Mooney-Rivlin, explained in 5.4.2.

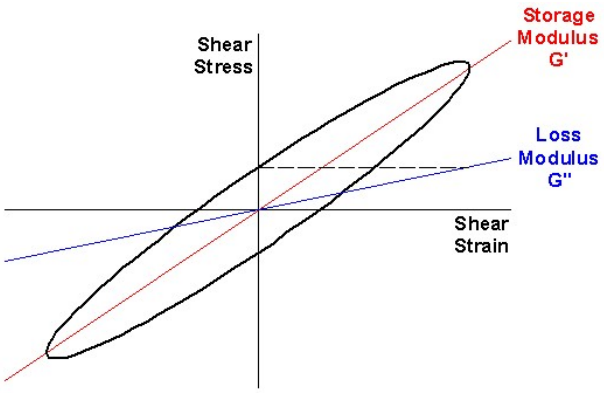

Figure 5.7: stress-strain cycle for rubber. The ellipse represents a set of empirical measures.

5.4 Structure equations

The equations of the tire, the structure, come from the conservation of momentum and material models for hyper- and viscoelasticity.

5.4.1 Conservation of momentum

With Newton's second law we have $\boldsymbol{F} = m\boldsymbol{a} = m\frac{\partial^2 \boldsymbol{d}}{\partial t^2}$ where $\boldsymbol{d} = \boldsymbol{x} - \boldsymbol{X}$ contains the displacements of the rubber. When considering a moving infinitesimal tire element, it can experience body and/or surface forces.

- Body forces, which act directly on the volumetric mass of the tire element. These forces "act at a distance"; examples can be gravitational and electromagnetic forces. In case of hydroplaning only gravitation is taken into account.
- Surface forces, which act directly on the surface of the tire element. They are due only to two sources.
  - The pressure distribution acting on the surface, imposed by the outside fluid surrounding the tire element.
  - The shear and normal stress distributions acting on the surface, also imposed by the outside fluid by means of friction.

Let $\boldsymbol{f}$ denote the body force per unit mass in $[\frac{N}{kg}]$, then

$$\text{body force on element} = \rho \boldsymbol{f} dxdydz.$$

From Figure 4.4 it follows that

$$\begin{aligned}
\text{net surface force in } x \text{ direction} &= \left[p - \left(p + \frac{\partial p}{\partial x}dx\right)\right] dydz + \left[\left(\tau_{xx} + \frac{\partial \tau_{xx}}{\partial x}dx\right) - \tau_{xx}\right] dydz \\
&+ \left[\left(\tau_{yx} + \frac{\partial \tau_{yx}}{\partial y}dy\right) - \tau_{yx}\right] dxdz + \left[\left(\tau_{zx} + \frac{\partial \tau_{zx}}{\partial z}dz\right) - \tau_{zx}\right] dxdy \\
&= \left[-\frac{\partial p}{\partial x} + \frac{\partial \tau_{xx}}{\partial x} + \frac{\partial \tau_{yx}}{\partial y} + \frac{\partial \tau_{zx}}{\partial z}\right] dxdydz
\end{aligned}$$

The $\star + \frac{\partial \star}{\partial \{x,y,z\}} d\{x,y,z\}$ terms are again from Taylor expansions, analogous with the decuction in 4.3.3.

With analogy in y and z direction and 4.4, the total force becomes

$$\boldsymbol{F} = \left[\rho \boldsymbol{f} - \boldsymbol{\nabla} p + \boldsymbol{\tau}^T \boldsymbol{\nabla}\right] dxdydz \tag{5.1}$$

With $\boldsymbol{F} = m\boldsymbol{a}$ and noting that $m = \rho dxdydz$, $\boldsymbol{a} = \frac{\partial^2 \boldsymbol{d}}{\partial t^2}$, $\boldsymbol{f} = \boldsymbol{g}$ and for the stress tensor $\boldsymbol{\tau} = \boldsymbol{\tau}^T$ we get

$$\begin{aligned}
\left[\rho \boldsymbol{g} - \boldsymbol{\nabla} p + \boldsymbol{\tau} \boldsymbol{\nabla}\right] dxdydz &= \rho \frac{\partial^2 \boldsymbol{d}}{\partial t^2} dxdydz \\
\rho \boldsymbol{g} - \boldsymbol{\nabla} p + \boldsymbol{\tau} \boldsymbol{\nabla} &= \rho \frac{\partial^2 \boldsymbol{d}}{\partial t^2}
\end{aligned} \tag{5.2}$$

where the deviatoric stress $\boldsymbol{\tau}$ is related to the material model used for rubber. As the Goodyear material model for rubber is classified, the simpler Mooney-Rivlin material model is used throughout this report.

5.4.2 Mooney-Rivlin

Elastic materials for which the work is independent of the load path are said to be hyperelastic or Green elastic materials. Hyperelastic materials are characterised by the existence of a strain (or stored) energy function that is a potential for stress

$$\boldsymbol{\tau} = 2\frac{\partial}{\partial \boldsymbol{C}} \psi(\boldsymbol{C}) \tag{5.3}$$

where ψ is the strain energy potential and $\boldsymbol{C} = \boldsymbol{F}^T \boldsymbol{F}$ the right Cauchy-Green deformation tensor. A consequence of the existence of a strain energy function is that the work done on a hyperelastic material is independent of the deformation path. This is confirmed by

$$\frac{1}{2} \int_{\boldsymbol{C}_1}^{\boldsymbol{C}_2} \boldsymbol{\tau} : d\boldsymbol{C} = \psi(\boldsymbol{C}_2) - \psi(\boldsymbol{C}_1)$$

This behaviour is approximately observed in many rubber-like materials [2].

Given isotropy and additive decomposition of the deviatoric and volumetric strain energy contributions

in the presence of incompressible or almost incompressible behaviour, the strain energy potential can be written as

$$\exists f, g \quad \ni \quad \psi = \underbrace{f(\bar{I}_1 - 3, \bar{I}_2 - 3)}_{\text{deviatoric}} + \underbrace{g(J_{\text{element}} - 1)}_{\text{volumetric}}$$

with

$$\begin{aligned} \bar{I}_1 &\equiv \text{trace}(\boldsymbol{B}) \\ \bar{I}_2 &\equiv \frac{1}{2}(\bar{I}_1^2 - \text{trace}(\boldsymbol{B}^2)) \\ \boldsymbol{B} &\equiv \boldsymbol{F}\boldsymbol{F}^T \\ J_{\text{element}} &= \frac{J}{J_{\text{thermal}}} \\ J_{\text{thermal}} &= (1 + \epsilon_{\text{thermal}})^3 \end{aligned}$$

where linear thermal expansion $\epsilon_{\text{thermal}}$ follows from the temperature and the isotropic thermal expansion coefficient defined by the user. The $\bar{I}_1$ and $\bar{I}_2$ are called the first and second invariants of the left Cauchy-Green deformation tensor $\boldsymbol{B}$ respectively. The J, J_{element} and J_{thermal} are the total, elastic and thermal volume strain.

Setting [21]

$$g = \sum_{i=1}^{N} \frac{1}{D_i}(J_{\text{element}} - 1)^{2i}$$

and expanding f in a Taylor series, it follows that

$$\psi = \sum_{i+j=1}^{N} C_{ij}(\bar{I}_1 - 3)^i(\bar{I}_2 - 3)^j + \sum_{i=1}^{N} \frac{1}{D_i}(J_{\text{element}} - 1)^{2i} \quad , N \in \mathbb{N}.$$

The N is usually not taken higher than two when both the first and second invariants are taken into account. The coefficients C_{ij} and D_i are functions of the temperature defined by the user. The D_i determine the compressibility of the material: if all D_i are zero, the material is fully incompressible. If $D_1 = 0$, then $D_i = 0 \quad \forall i$. Regardless of the value of N, the initial shear and bulk modulus G and K depend only on the polynomial coeffcients of order $N = 1$:

$$G = 2(C_{10} + C_{01}) \quad K = \frac{2}{D_1}.$$

If $N = 1$ the Mooney-Rivlin form is recovered

$$\psi = C_{10}(\bar{I}_1 - 3) + C_{01}(\bar{I}_2 - 3) + \frac{1}{D_1}(J_{\text{element}} - 1)^2 \tag{5.4}$$

which is an expansion of the Neo-Hookean form

$$\psi = C_{10}(\bar{I}_1 - 3) + \frac{1}{D_1}(J_{\text{element}} - 1)^2. \tag{5.5}$$

This form is the simplest hyperelastic model. Surprisingly, its representation resembles the model for an ideal gas: the Neo-Hookean represents the Helmholtz free energy of a molecular network with Gaussian chain-length distribution [21]. Note that $\psi = \psi(\bar{I}_1(\boldsymbol{B}(\boldsymbol{F}(\boldsymbol{x}))), \bar{I}_2(\boldsymbol{B}(\boldsymbol{F}(\boldsymbol{x}))))$ and is thus a function of spatial coordinates $\boldsymbol{x}$.

5.4.3 Initial and boundary conditions

Considering (5.2)

$$\rho\frac{\partial^2 \boldsymbol{d}}{\partial t^2} = \rho\boldsymbol{g} - \boldsymbol{\nabla}p + \boldsymbol{\tau}\boldsymbol{\nabla}$$

three additional equations are provided. The dependent variables are $\boldsymbol{d}, \rho, p$ and $\boldsymbol{\tau}$. Displacement $\boldsymbol{d} = \boldsymbol{x} - \boldsymbol{X}$ is a function of $\boldsymbol{x}$, since the material coordinates $\boldsymbol{X}$ of the tire are known. Density of rubber ρ is determined by the volume change $J \equiv \det(\boldsymbol{F}) = \det(\frac{\partial \boldsymbol{x}}{\partial \boldsymbol{X}})$ thus $\rho = \rho(\boldsymbol{x})$. Pressure p stems from the fluid equations and in 5.4.2 it was determined that $\boldsymbol{\tau}$ is also a function of $\boldsymbol{x}$. Herewith, three equations and three variables are added.

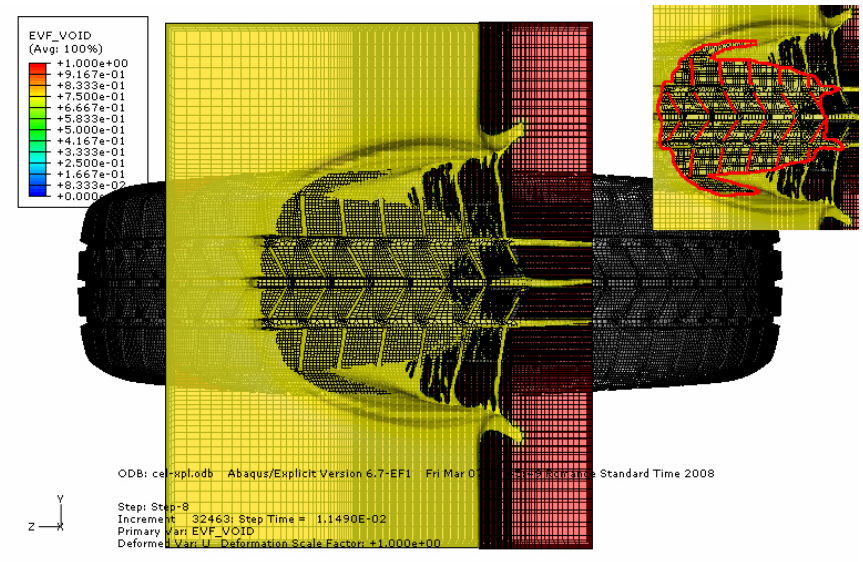

Figure 5.8: boundaries.

From (5.2) it follows that two ICs and one BC over the whole boundary are needed for a unique solution. Where the tire is in contact with air, the deformation and velocity can be assumed $\forall t \quad \boldsymbol{d} = \mathbf{0} \wedge \frac{\partial \boldsymbol{d}}{\partial t} = \mathbf{0}$. For the footprint, cf. Figure 5.8, the displacement and velocity follow from the tire being in a steady state rolling (SSR) situation. A quantitative approach of SSR is beyond the scope of this report. For contact with the fluid, the displacement follows from stress of the fluid. Summarised in formula

$$\boldsymbol{d}|_{t=t_0} \wedge \frac{\partial \boldsymbol{d}}{\partial t}|_{t=t_0} \quad \ni \quad \begin{cases} \boldsymbol{d} = \mathbf{0}, \frac{\partial \boldsymbol{d}}{\partial t} = 0 & \Gamma_{\text{air}} \\ \text{SSR} & \Gamma_{\text{tarmac}} \end{cases} \tag{5.6}$$

$$\boldsymbol{d} \quad \ni \quad \begin{cases} \boldsymbol{d} = \mathbf{0} & \Gamma_{\text{air}} \\ \text{SSR} & \Gamma_{\text{tarmac}} \\ \text{fluid stress} & \Gamma_{\text{interface}} \end{cases} . \tag{5.7}$$

The BC for the pressure p was treated in 4.7.3.

5.4.4 Obscurities

Lack of information as described in 4.9 has lead to postponement of stating the weak formulation and usage of FEM for the structure equations. A thorough treatment is to follow in the Master thesis.

Chapter 6

Fluid-structure interaction

6.1 Introduction

A problem involving fluid flow interacting with structures is a fluid-structure interaction problem, FSI in short. Flow for instance around or alongside a structure, influencing or interacting with the physical quantities of the structure and vice versa. From the fluid's point of view the pressure, velocity and temperature are inlfuenced. From the structure's point of view the displacement, temperature and electrical properties (see Figure 6.1). These are fluid-structure interaction problems. The fluid flow usually undergoes large deformations but also the structure does not need to be fixed and rigid but can be moving and deformable. Examples are sloshing of tanks in launchers, limit cycle oscillations of wings, instabilities in the wind interaction with cable stayed bridges, the inflation of an airbag and of course hydroplaning.

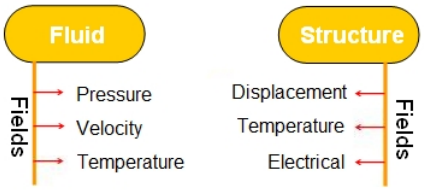

Figure 6.1: fluid-structure interaction.

These problems can be handled nowadays thanks to the increase of computing power and advances in numerical methods in the last decade. Where classically, FSI problems have been analyzed using cumbersome analytical methods, CFD and FEM methods have taken over [3].

FSI problems can be divided into the following parts:

- monolithic or partitioned solver
- mesh fluid
- mesh structure
- coupling of non-matching meshes
- interface tracking
- space discretisation
- time discretisation.

6.2 Monolithic or partitioned?

In order to come to an approach for the development of an efficient FSI solver, the first choice that has to be made is whether to develop a monolithic or a partitioned solver. A monolithic solver aims at putting all the necessary components (the physical modelling, discretisations and solution algorithms) into a single computational model and solver, see Figure 6.2. It solves the set of fluid and structure equations simultaneously. Although some papers have appeared on monolithic solvers, the general opinion seems to be that monolithic solvers are not practical: not only the implementation of different physical models within a single solution environment can be difficult, also the continuous effort of keeping the solver up-to-date with the latest developments in each research field may prove to be a daunting task. Therefor the popular approach is to develop a partitioned solver [1]. A partitioned solver treats each physical domain separately, see Figure 6.2. Hereby it can use existing solvers that can be developed and maintained indepently.

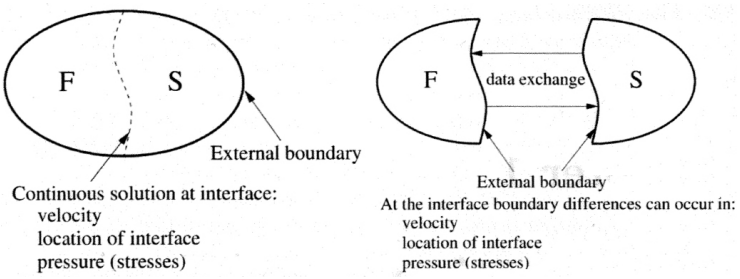

Figure 6.2: monolithic or partitioned? [1].

A partitioned FSI solver consists of a flow solver, a structure solver and a coupling algorithm that couples the solvers at the fluid-structure interface both in space and time. The coupling algorithm contains an interpolation method to transfer data from one system to the other and an iteration scheme to obtain a coupled solution that is within the desired accuracy.

Nevertheless, Abaqus' FSI solver is monolithic and thus solves the fluid and structure equations simultaneously.

6.3 Coupling non-matching meshes

Domain decomposition is a common way to speed up complex computations. The discrete meshes used in the different domains do not have to match at their common interface. This is also the case when different physical fields are involved such as in fluid-structure interaction computations. Exchange of information over this interface is therefor no longer trivial [4].

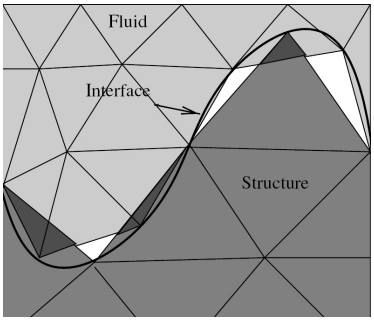

Figure 6.3: non-matching meshes in 2D [3].

Computers and numerical methods have significantly advanced over the past decade such that the simulation of complex physical problems and even multi-field problems has become feasible. For an efficient computation of these problems parallel computing is a must. A common way to perform these parallel computations is by domain decomposition. The total domain is subdivided into smaller domains on which the problem is computed in parallel and interaction effects between the domains are treated as boundary conditions at their common interfaces. Especially when different physical aspects are involved the meshes of the different domains do not have to match at their common interface. This means that the discrete interface between the domains may not only be non-conforming, but there may also be gaps and/or overlaps between the meshes. The exchange of data over the discrete interface becomes then far from trivial. In Figure 6.3 a 2D example of a non-matching discrete interface between a flow and structure domain is shown. Another example is Figure 6.4.

For information transfer FSI computations require that pressure loads are transmitted from the fluid side of the fluid-structure interface to the structural nodes on that interface. Also, once the motion of the structure has been determined, the motion of the fluid mesh points on the interface has to be imposed. In FSI simulations generating matching meshes at the fluidstructure interface is usually not desirable, because the flow generally requires a much finer mesh than the structure and, due to the modularity of the partitioned coupling technique, different teams may take care of the different solvers. When meshes are non-matching, an interpolation/projection step has to be carried out to enable transfer of information between the two domains.

There are several criteria which such a data exchange or coupling method ideally should satisfy. The most important are

- global conservation of energy over the interface
- global conservation of loads over the interface
- accuracy
- conservation of the order of the coupled solvers

- efficiency, which is defined as a ratio between accuracy and computational costs.

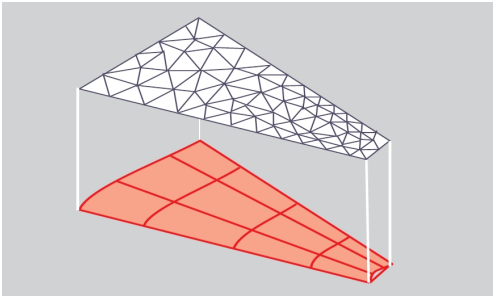

Figure 6.4: non-matching meshes [3].

The simplest and fastest way to perform the information transfer is to obtain the information from the closest point in the other mesh, the so-called nearest neighbour interpolation. However, this only provides satisfactory results if the two grids are almost matching. A more accurate way of handling the data transfer is by projection, cf. Figure 6.5. To obtain information from the other mesh, a point can be orthogonally projected on that mesh and the information in that projection point can be used in the original point. Similarly, a whole element can be orthogonally projected on the other mesh and the size of the area of intersection can then be used to define to what degree the values of that element have to be taken into account. Note that the perspective in Figure 6.5 does not imply the surfaces being seperated (no contact). The seperation is only for comprehension of the projection. The third way to exchange data is using spline based methods. These are often applied in interpolation schemes in finite element methods. An example is radial basis functions interpolation.

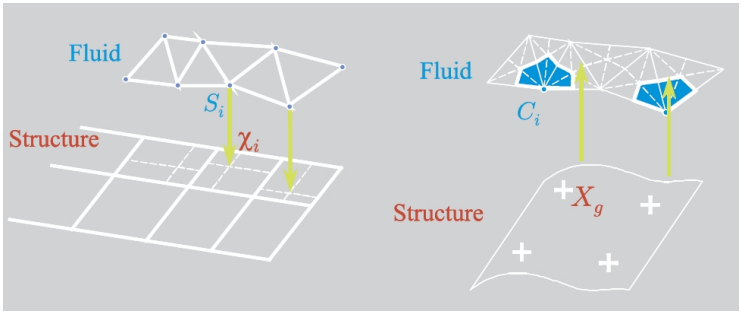

Figure 6.5: information transfer by means of projection [3].

In the CEL method the penalty method is used to enforce the rolling contact. Coupling non-matching meshes is an issue here. At this time this is still under investigation.

6.4 Interface tracking

Abaqus' CEL method for treating FSI problems contains an interface tracking method like every FSI solver. In this case the volume of fluid (VOF) method is used [9]. VOF is a method based on the concept of a fractional volume of fluid per mesh cell.

Free boundaries are considered to be surfaces on which discontinuities exist in one or more variables. Examples are free surfaces, material interfaces, shock waves and, like in our case, interfaces between fluid and deformable structures. Three types of problems arise in the numerical treatment of free boundaries:

1. discrete representation
2. evolution in time
3. imposing boundary conditions on them.

Considering a cell of a mesh it is customary to use only one value for each dependent variable defining the fluid state. The use of several points in a cell to define the region occupied by the fluid, therefor, seems unnesecarily excessive. Suppose that we define a function $F \in [0, 1]$ whose value is unity at any point

occupied by fluid and zero otherwise. The average value of F in a cell would then represent the fractional volume of the cell occupied by fluid. In particular, a unit value of F would correspond to a cell full of fluid, while a zero value would indicate that the cell contained no fluid. Accordingly, $\forall t \in [t_0, \infty)$

$$(FV)_{i,j,k}(t) = \int\limits_{V_{i,j,k}} F(x,y,z,t)dV \quad \Leftrightarrow \quad F_{i,j,k} = \frac{\int\limits_{V_{i,j,k}} F(x,y,z,t)dV}{V_{i,j,k}} \tag{6.1}$$

with F the volume fraction and V the volume in $[m^3]$. Cells with $F \in (0,1)$ must contain a free surface. In this way, VOF only uses one value per cell which is consistent with the requirements of all other dependent variables.

From conservation of mass, the conservation of volume follows. Conservation of volume implies conservation of F. Accordingly, it is expressed as a similar way. Recall that for conservation of a material property F

$$\begin{array}{rcl} \text{net flow out } F & & \text{time rate of} \\ \text{of control volume} & = & \text{decrease of } F \\ \text{through surface} & & \text{inside control volume} \end{array} .$$

This yields

$$\frac{\partial}{\partial t} \iiint\limits_V F dV = - \iint\limits_S F\boldsymbol{v} \cdot \boldsymbol{n} dS.$$

For VOF methods an Eulerian frame is used and thus V is independent of time t. Herewith and the divergence theorem applied on the right hand side it follows that

$$\iiint_V \left[\frac{\partial F}{\partial t} + \boldsymbol{\nabla} \cdot F\boldsymbol{v} \right] = 0 \tag{6.2}$$

called the advection equation in integral form [20]. The velocity $\boldsymbol{v}$ stems from the fluid equations. Typically in interface tracking methods, an important issue is the prevention of loss of fluid. The used discretisation scheme plays a role here.

Notice that in case of incompressibility, (4.28) yields $\boldsymbol{\nabla} \cdot F\boldsymbol{v} = \boldsymbol{\nabla} F \cdot \boldsymbol{v} + F\boldsymbol{\nabla} \cdot \boldsymbol{v} = \boldsymbol{\nabla} F \cdot \boldsymbol{v}$ and thus

$$\iiint_V \left[\frac{\partial F}{\partial t} + \boldsymbol{\nabla} F \cdot \boldsymbol{v} \right] = 0.$$

Apart from the evolution of F, it is still unknown where the fluid is in each cell. This information is needed for the reconstruction of the interface.

There are several interface reconstruction methods, both first and second order accurate in space. In [12], a design criteria is proposed, namely that when lines in two dimensions or planes in three dimensions are reproduced exactly, the method is second order accurate. The authors introduce two algorithms based on least squares, that are second order accurate. Furthermore, methods like simple line and piecewise linear interface calculation (SLIC and PLIC) are recalled, cf. Figure 6.6. Abaqus' CEL method makes use of a PLIC [25]. This usage will be explained thoroughly in the Master thesis.

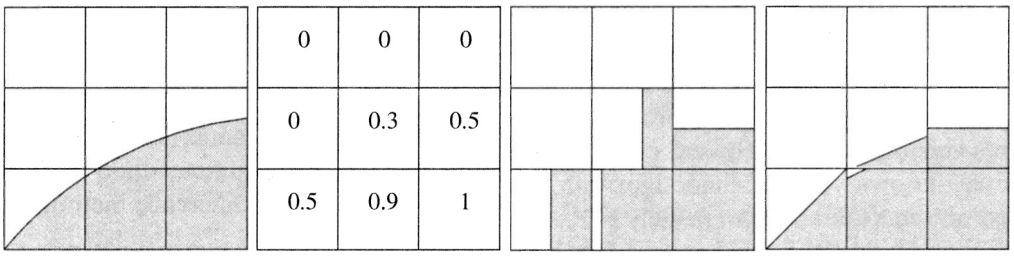

(a) True surface. (b) Volume fractions. (c) SLIC. (d) PLIC.

Figure 6.6: interface reconstruction [12].

Chapter 7

Piston benchmark

7.1 Introduction

The CEL method of Abaqus needs to be tested on accuracy, computational speed and plausibility of the produced solution. This kind of testing is also referred to as benchmarking. Herefor, we need to treat a FSI example problem. Preferably a problem with the solution already known. The ideal case being that an analytical solution is known. A well known example problem is the piston problem [1, 16]. This is an one-dimensional problem whereof the analytical solution is known. The piston problem is explained. Typical FSI issues occur.

7.2 Model

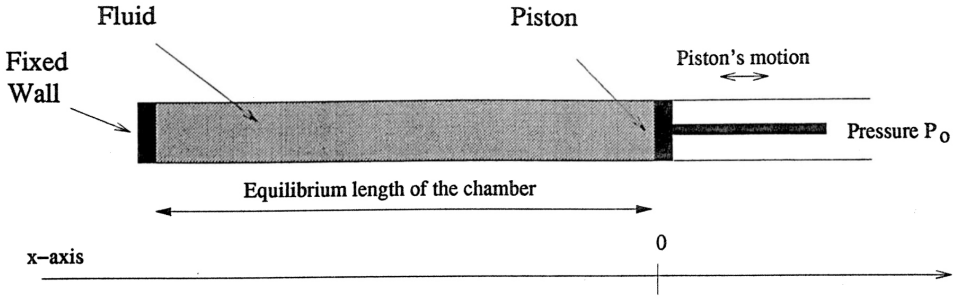

Figure 7.1: the piston and the fluid-filled one-dimensional chamber [16].

Consider the one-dimensional flow of a perfect gas in a chamber closed by a moving piston, cf. Figure 7.1. The equilibrium state is defined by a uniform pressure p_0 in- and outside of the chamber, a uniform gas density ρ_0 in the chamber, where the gas is nonmoving $u_0 = 0$ and by a stationary chamber length L. The one-dimensional flow in the chamber is governed by the compressible Euler equations without body forces

$$\begin{aligned} \frac{\partial}{\partial t}\rho + \frac{\partial}{\partial x}(\rho u) &= 0 \\ \frac{\partial}{\partial t}(\rho u) + \frac{\partial}{\partial x}(\rho u^2 + p) &= 0 \end{aligned} \tag{7.1}$$

the one-dimensional form of (4.26).

The position, speed and acceleration of the piston are respectively denoted by $L + q, \dot{q}, \ddot{q}$ with q the deviation of the piston from its equilibrium L. Calling m, d and k the mass in $[kg]$, internal damping in $[\frac{kg}{s}]$ and the stiffness in movement in $[\frac{N}{m}]$ (coming from a spring for instance) of the piston respectively, the force equilibrium $\sum \boldsymbol{F} = m\boldsymbol{a}$ for the piston can be deduced:

$$\begin{aligned} \underbrace{p(L+q(t),t)A - d\dot{q}(t)}_{\text{inside forces}} \underbrace{-kq(t) - p_0 A}_{\text{outside forces}} &= m\ddot{q}(t) \\ m\ddot{q}(t) + d\dot{q}(t) + kq(t) &= (p(L+q(t),t) - p_0)A \end{aligned} \tag{7.2}$$

where $p(L + q(t), t)$ is the internal pressure at the piston and A the surface of the piston. It is assumed that the outer pressure p_0 remains constant. The ICs are $q(0) = q_0$ and $\dot{q}(0) = \dot{q}_0$.

For uniqueness of a solution of (7.1) an IC and BC are needed per variable. The ICs are $\rho(x, 0) = \rho_0$ and $u(x, 0) = 0$ because at time $t_0 = 0$ the density is equal to the reference density and the velocity in the gas is still zero. The BCs of the fluid are $(\rho u)(0, t) = 0$ at the fixed wall and $u(L + q, t) = \dot{q}$ at the piston, which expresses that the fluid velocity is equal to the piston speed $L + q$. In this way the problem is still not defined properly. A full benchmark is to follow.

Chapter 8
Research proposal

To further investigate the feasibitlity of Abaqus' CEL method for the modelling of hydroplaning, certain areas need to be researched.

A focal point is the coupling of the non-matching meshes. The structure mesh adapts slightly to the fluid mesh and vice versa using the penalty method in balanced form. Is this done properly? Purpose hereof is ensuring adequate transfer of information over the interface. Surface reconstruction algorithms in combination with VOF can also differ. Comparison with a self-constructed Matlab model would be appropriate.

When lack of knowledge about the theory behind Abaqus is encountered, benchmarking is an alternative. Problems wereof the analytical or discretized solution is a priori information can reveal properties of Abaqus.

To approximate the behaviour of incompressible fluids, Abaqus uses the compressible form of the governing equations in combination with low compressibility or high bulk modulus. The bulk modulus relates to the stable timestepsize inversely. A higher bulk modulus, and thus a better approximation of incompressibilty, results in a smaller stable timestepsize, and therefor longer calculation time. Calculation time is in the order of days and so the bulk modulus should be carefully chosen. Furtermore, experience is that the compressible and incompressible form are very distinct, especially in mathematical sense. Thus, it is of relevance to judge the considering approximation in this sense.

In agreement with the above mentioned, the research proposal in points of research:

1. coupling of non-matching meshes
2. penalty method
3. infromation transfer over interface
4. surface reconstruction
5. benchmarks
6. compressible $\rightarrow$ incompressible
7. bulk modulus $\leftrightarrow$ stable timestepsize.

Bibliography

[1] A.H. van Zuijlen, *Fluid-structure interaction simulations, effcient high order time integration of partitioned systems*, PhD thesis, TU Delft, Delft, 2006.

[2] T. Belytschko, W.K. Liu, and B. Moran, *Nonlinear finite elements for continua and structures*, Wiley, West Sussex, 2007.

[3] H. Bijl, A.H. van Zuijlen, A. de Boer, and D.J. Rixen, *Fluid-structure interaction.* Delft institutes of aerospace and mechanical engineering, Delft, 2007.

[4] A. de Boer, A.H. van Zuijlen, and H. Bijl, *Review of coupling methods for non-matching meshes*, Computer Methods in Applied Mechanics and Engineering, 196 (2006), pp. 1515–1525.

[5] D.F. Parker, *Fields, flows and waves*, Springer, London, 2003.

[6] D.J. Benson, *Computational methods in Lagrangian and Eulerian hydrocodes*, Comput. Methods Appl. Mech. Eng., 99 (1992), pp. 235–394.

[7] D.S. Stewart, S. Yoo, and B.L. Wescott, *High-order numerical simulation and modelling of the interaction of energetic and inert materials*, Combustion theory and modelling, 11 (2007), pp. 305–332.

[8] R. Haberman, *Applied partial differential equations with Fourier series and boundary value problems*, Pearson Prentice Hall, New Jersey, fourth ed., 2004.

[9] C. Hirt and B. Nichols, *Volume of fluid (VOF) method for the dynamics of free boundaries*, Journal of Computational Physics, 39 (1981), pp. 201–225.

[10] J. Donea, A. Huerta, J.P. Ponthot, and A. Rodríguez-Ferran, *Arbitrary Lagrangian-Eulerian methods*, Encyclopedia of computational mechanics, Volume 1: fundamentals (2004).

[11] J.D. Anderson jr., *Computational fluid dynamics, the basics with applications*, McGraw-Hill Inc., Singapore, 1995.

[12] J.E. Pilliod Jr. and E.G. Puckett, *Second-order accurate volume-of-fluid algorithms for tracking material interfaces*, J. Comput. Phys., 199 (2004), pp. 465–502.

[13] J.J. Kalker, *Three-dimensional elastic bodies in rolling contact*, Kluwer Academic Publishers, Dordrecht, 1990.

[14] K.H. Brown, S.P. Burns, and M.A. Christon, *Coupled Eulerian-Lagrangian Methods for Earth Penetrating Weapon applications*, U.S. Department of Commerce, (2002).

[15] M.A. Meyers, *Dynamic behaviour of materials*, Wiley, New York, 1994.

[16] S. Piperno, *Simulation numérique de phénomènes d'interaction fluide-structure*, PhD thesis, École nationale des ponts et chaussées, Champs-sur-Marne, 1995.

[17] G. Post, *Applied functional analysis*, Delft, 2000.

[18] R.A. Adams, *Calculus: a complete course*, Pearson Addison Wesley, Toronto, sixth ed., 2006.

[19] R.C. Hibbeler, *Mechanics of materials*, Pearson Prentice Hall, Singapore, sixth ed., 2005.

[20] R.J. Leveque, *Finite volume methods for hyperbolic problems*, Cambridge University Press, Cambridge, 2002.

[21] Simulia, *Abaqus version 6.7-EF manual*, Simulia, Dassault Systèmes, United States of America, 2007.

[22] Simulia Benelux support staff member, *G. Kloosterman.*

[23] S.K. Clark, *Mechanics of pneumatic tires*, U.S. Government Printing Office, Washington, revised ed., 1975.

[24] E. van Groesen and J. Molenaar, *Advanced modelling in science.* UT Twente, Enschede, 2007.

[25] W.J. Rider and D.B. Kothe, *Reconstructing volume tracking*, J. Comput. Phys., 141 (1998), pp. 112–152.

Straight hydroplaning test.